



# Environmental and Hydrological Changes of Lake Coatetelco in Central Mesoamerica (Southwest Mexico) Over the Holocene and Comparison With Climatic Forcing

Oscar Agesandro García-Arriola<sup>1\*</sup>, Priyadarsi D. Roy<sup>2\*</sup>, Irma Gabriela Vargas-Martínez<sup>3</sup>, Ma. Patricia Giron-García<sup>2</sup>, Jason H. Curtis<sup>4</sup>, Isabel Israde-Alcantara<sup>5</sup> and Jesús David Quiroz-Jimenez<sup>6</sup>

## OPEN ACCESS

### Edited by:

G. Lynn Wingard,  
Florence Bascom Geoscience Center,  
United States Geological Survey  
(USGS), United States

### Reviewed by:

Liseth Pérez,  
Technische Universität Braunschweig,  
Germany  
Jessica Rodysill,  
United States Geological Survey  
(USGS), United States

### \*Correspondence:

Oscar Agesandro García-Arriola  
agess301290@hotmail.com  
Priyadarsi D. Roy  
priyadarsi1977@gmail.com

### Specialty section:

This article was submitted to  
Paleoecology,  
a section of the journal  
Frontiers in Ecology and Evolution

Received: 05 November 2021

Accepted: 23 May 2022

Published: 14 June 2022

### Citation:

García-Arriola OA, Roy PD,  
Vargas-Martínez IG, Giron-García MP,  
Curtis JH, Israde-Alcantara I and  
Quiroz-Jimenez JD (2022)  
Environmental and Hydrological  
Changes of Lake Coatetelco  
in Central Mesoamerica (Southwest  
Mexico) Over the Holocene  
and Comparison With Climatic  
Forcing. *Front. Ecol. Evol.* 10:809949.  
doi: 10.3389/fevo.2022.809949

<sup>1</sup> Posgrado en Ciencias del Mar y Limnología, Universidad Nacional Autónoma de México, Ciudad de México, Mexico, <sup>2</sup> Instituto de Geología, Universidad Nacional Autónoma de México, Ciudad de México, Mexico, <sup>3</sup> Carrera de Ingeniería Geológica, Facultad de Ingeniería, Universidad Nacional Autónoma de México, Ciudad de México, Mexico, <sup>4</sup> Department of Geological Sciences, University of Florida, Gainesville, FL, United States, <sup>5</sup> Instituto de Investigaciones en Ciencias de la Tierra, Universidad Michoacana de San Nicolás de Hidalgo, Morelia, Mexico, <sup>6</sup> Área Académica de Ciencias de la Tierra y Materiales, Universidad Autónoma del Estado de Hidalgo, Pachuca, Mexico

Elemental composition of the inorganic fraction, carbon isotopes, and C/N of organic matter from a new radiocarbon-dated sedimentary sequence collected from Lake Coatetelco (960 m asl) extend information about the environmental and hydrological conditions of central Mesoamerica from the earliest Holocene to the interval of first human settlements in the lake vicinity and nearby streams. Proxy-based reconstructions of erosion/runoff (Ti), water column salinity (CaCO<sub>3</sub>), sediment–water interactions (PIA), and provenance of organics ( $\delta^{13}\text{C}_{\text{org}}$  and C/N) showed similarities with the summer insolation modulated ITCZ position between  $\sim 11.5$  and 4.2 cal ka BP, and more frequent ENSO between  $\sim 4.2$  and 2.1 cal ka BP. After a possible depositional hiatus between  $\sim 11.2$  and 10.2 cal ka BP, the moderate-to-extremely altered sediments were deposited with enhanced erosion/runoff during the wetter  $\sim 10.2$ –6 cal ka BP and the organic matter was dominantly autochthonous. Comparison of  $\delta^{13}\text{C}_{\text{org}}$  and C/N suggested that the contribution of C<sub>4</sub> plants to organic matter increased over the drier  $\sim 6$ –4.2 cal ka BP. Sediments representing this middle- Holocene drought-like condition showed geochemical similarity with sediments of the Post-Classic drought ( $\sim 1$ –0.4 cal ka BP), coeval with abandonment of the Xochicalco culture. Variation in seasonal insolation at orbital scales might have forced frequent droughts between  $\sim 6$  and 4.2 cal ka BP and the ENSO related short-lived storms possibly led to an unstable hydroclimate after  $\sim 4.2$  cal ka BP when the first Olmec settlements commenced in the region. Dissimilarity between this lacustrine archive and speleothems from southwest Mexico for the later part of the Holocene reflected different sensitivities of the geological records to seasonal and annual precipitation.

**Keywords:** paleoclimate, middle Holocene drought, geochemistry, carbon isotopes, lacustrine record, Mexico

## INTRODUCTION

The applications of complementary paleoenvironmental and paleohydrological tools in geological registers have systematically reconstructed the responses of ecosystems and depositional environments to global climate change (Haug et al., 2003; Hodell et al., 2005; Metcalfe et al., 2010; Bernal et al., 2011; Bhattacharya et al., 2015; Roy et al., 2017, 2020; Aragón-Moreno et al., 2018; Park et al., 2019). Clastic-allochthonous components of sedimentary archives have responded with a lower time lag to the centennial-to-millennial-scale events of hydroclimate compared to the biological components (e.g., Jennerjahn et al., 2004). Both the inorganic and organic components, however, have successfully deciphered the relationship between climate and several pre-Columbian cultures as well as the influences of oceanic-atmospheric forcing on Mesoamerica that extends over central and southern Mexico, and most of Central America including Belize, Guatemala, El Salvador, Honduras, Nicaragua, and Costa Rica (Figure 1). The flourishing and demise of urban centers in this region with variable geology, geomorphology, and climate were concurrent with the pluvial conditions and droughts since the Pre-Classic Period of the late Holocene (Lachniet et al., 2017). The abandonment of residential structures and densely populated urban centers during the late Classic and early Post Classic droughts highlighted the possible role of climate change on political unrest. Decline of the Teotihuacan culture occurred simultaneously as the Rincon de Parangueo maar record suggested abandonment of agriculture (Park et al., 2019). Demographic disaster of densely populated urban centers of Maya across the Yucatan Peninsula occurred during almost cyclic and decadal-to-subdecadal-scale intervals of scarce precipitation (Curtis et al., 1996; Hodell et al., 2001). An arid interval, documented in sediments of the Aljojuca maar, was contemporary to demise of the Cantona culture (Bhattacharya et al., 2015). Records from the Lago Verde and Los Petenes on the Gulf of Mexico coast provided evidence of abandoned agriculture by the Maya societies during these droughts (Lozano-García et al., 2007; Roy et al., 2017). The frequent droughts identified in the latest Holocene geological deposits of eastern Mesoamerica were possibly regionally extensive as the sedimentary deposits of Laguna Juanacatlán in western Mesoamerica also registered a reduction in the amount of precipitation (Metcalfe et al., 2010). Sediments of Lake Coatetelco in central Mesoamerica have decoded the hydroclimate during the development of an important urban center of the Xochicalco culture. Arid conditions and enhanced aeolian activity in the watershed of Lake Coatetelco between  $\sim 1$  and  $0.4$  cal ka BP (944–1096 CE) were coeval with the demise of Xochicalco at  $\sim 950$ –1100 CE (Roy et al., 2020). Anthropogenic activities by these settled societies, however, modified the surrounding terrestrial as well as aquatic environments and led to poor preservation as well as perturbation of the sedimentary archives (Carrillo-Bastos et al., 2010; Aragón-Moreno et al., 2012; Lozano-García et al., 2013; Bhattacharya et al., 2015; Vázquez-Castro et al., 2019). For example, the deforestation and other agricultural activity by the Maya were indicated by the preserved pollen grains of disturbance taxa and maize as well as charcoal particles in

geological registers of the eastern Mesoamerica (Lozano-García et al., 2007; Aragón-Moreno et al., 2012; Bhattacharya et al., 2015). Similarly, the traditional agricultural practices in central Mesoamerica modified deposits of the Basin of Mexico, and the sediments from different geological provenances were mixed on a shallow lakebed for agriculture in western Mesoamerica by the Teuchitlán society of Guachimontones (Stuart, 2003; Vázquez-Castro et al., 2019).

The limitations posed by depositional hiatus and anthropogenic perturbations have been overcome with the help of high-resolution speleothem records as well as some well-preserved marine and lacustrine registers. They have constrained the cyclicity of decadal-to-subdecadal droughts as well as evaluated the forcing on heterogeneous hydroclimates before human occupation with minimal anthropogenic activities, i.e., over the early and middle Holocene (Haug et al., 2001; Medina-Elizalde et al., 2010; Metcalfe et al., 2010; Bernal et al., 2011; Roy et al., 2017). In central Mesoamerica, the hydroclimatic heterogeneity is reflected by dominant pine and oak with some *Alnus* and *Carpinus* in the surroundings of Lake Zirahuén until  $\sim 7$  cal ka BP, suggesting wetter conditions, and contemporaneous deposition of abundant authigenic carbonate in Lake Chalco indicating arid conditions (Lozano-García et al., 2013, 2015). Speleothems from Cueva del Diablo and Juxtlahuaca Caves, however, registered the decadal to centennial-scale variabilities within this interval of broader stable hydroclimate (Bernal et al., 2011; Lachniet et al., 2013). The arid events at  $\sim 10.3$  cal ka BP and  $\sim 8.2$  cal ka BP, indicating the disruptions of calcite deposition, were concurrent to the incidents of glacial melt water intrusions in the North Atlantic, and the enhanced aridity post  $\sim 4.3$  cal ka BP was contemporary to the phase of stronger El Niño Southern Oscillation (ENSO) (Bernal et al., 2011). More frequent ENSO and southward migration of the Inter-Tropical Convergence Zone (ITCZ) over the late Holocene also forced the change from semi-evergreen to dry tropical forest at the Rio Hondo delta in eastern Mesoamerica (Aragón-Moreno et al., 2018). However, the overall pattern of unsynchronous droughts across the Yucatan Peninsula underlined the need to evaluate the additional forcing such as the strength of the polar continental air mass, Caribbean low-level-jet, and tropical cyclones (Roy et al., 2017).

Even though the speleothems from central Mesoamerica (southwest Mexico) have already documented the paleomonsoon dynamics, the influences of climate change during the Holocene on other ecosystems, such as lakes which are an important source of surface water for agriculture and domestic usages, need separate attention. Studies on complementary geological registers can help to evaluate some of the existing discrepancies in this region. For example, the events of stalagmite growth interruptions at Juxtlahuaca Cave and Cueva del Diablo during the earliest Holocene were contemporary to an interval of more runoff and the presence of a dilute water column in the Lake Chalco in the Basin of Mexico (Bernal et al., 2011; Lachniet et al., 2013; Lozano-García et al., 2015). Here, we have extended the paleoenvironmental information for this region by generating a new and long record of paleohydrological conditions since the earliest Holocene and up to the first phase of settled societies

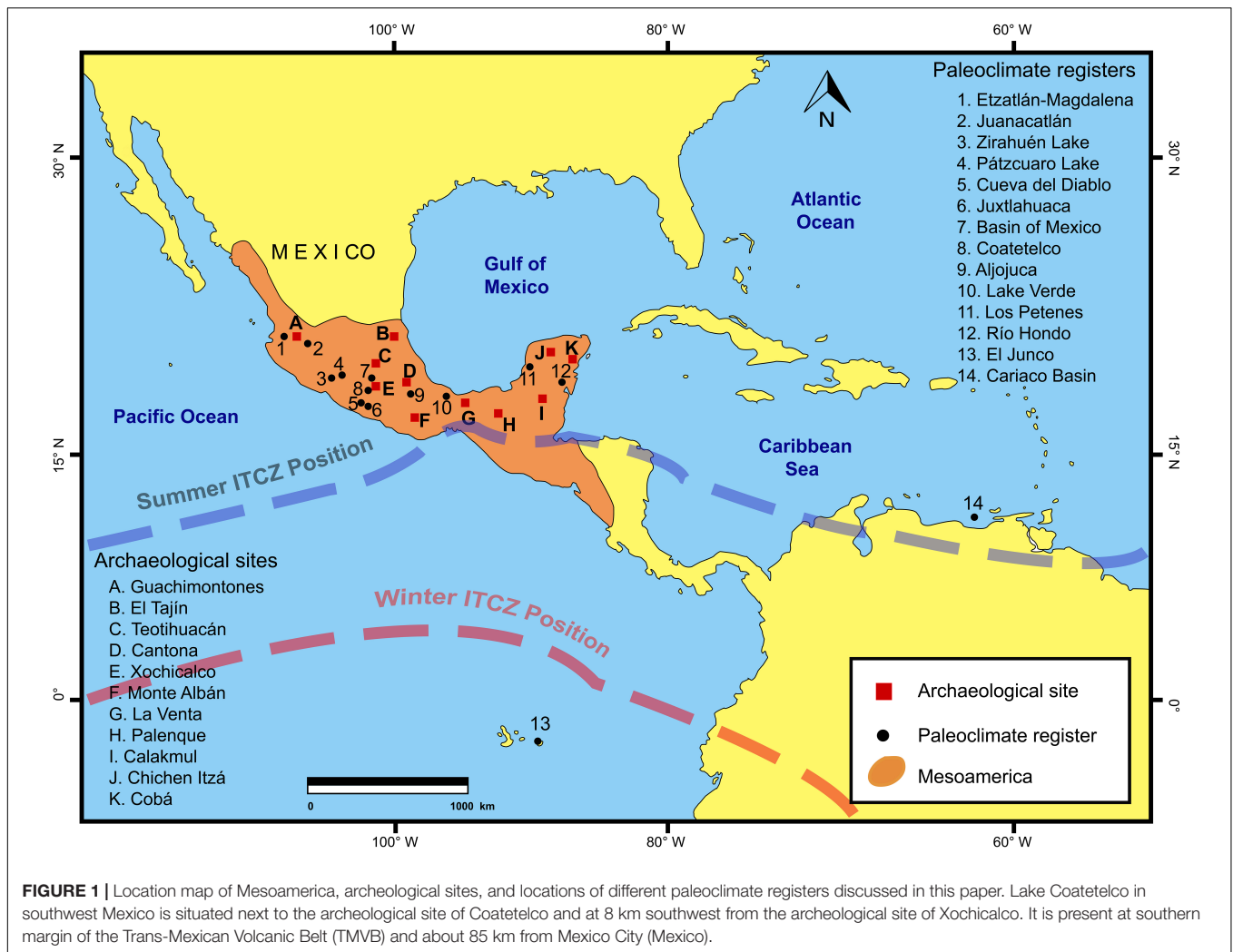


**FIGURE 1** | Location map of Mesoamerica, archeological sites, and locations of different paleoclimate registers discussed in this paper. Lake Coatetelco in southwest Mexico is situated next to the archeological site of Coatetelco and at 8 km southwest from the archeological site of Xochicalco. It is present at southern margin of the Trans-Mexican Volcanic Belt (TMVB) and about 85 km from Mexico City (Mexico).

(i.e., ~11.5–2.1 cal ka BP) from the geochemical composition of sediments deposited in the perennial Lake Coatetelco. Sub-millennial-scale variations in sources of the deposited organic matter and responses of precipitation/evaporation to global and/or regional climate change were inferred from carbon isotope composition ( $\delta^{13}\text{C}_{\text{org}}$ ) and C/N ratio of the bulk organic matter, abundances and chemical compositions of clastic and authigenic minerals, estimation of sediment-water interactions and provenances of siliciclastic fractions under the varying regimes of insolation, ITCZ position and ENSO activity.

## STUDY AREA, ARCHEOLOGY, AND HUMAN OCCUPATION

Lake Coatetelco is located at about 960 m above sea level in central Mesoamerica (Figure 1; 18°44' N, 99°20' W). It has a maximum length of 2 km and width of 1.5 km (NE-SW orientation) with a mean water depth below 0.5 m in 2017 (Gómez-Márquez, 2002; Díaz-Vargas et al., 2017). The water column salinity (TSD) in a total of different seasons of 2021CE

varied between 147 and 341 mg/l and pH between 5.9 and 8.4. The water-mineral saturation index (SI) for calcite suggested more supersaturation of calcite (SI: 0.77–0.83) in lake water of higher salinity (TDS: 331–341 mg/l) compared to lake water of lower salinity (SI: 0.40–0.62; TDS: 147–269 mg/l). This lake is present at the southern margin of the Trans-Mexican Volcanic Belt (TMVB), in the Morelos state of Mexico, located 85 km from Mexico City in southwest Mexico. Even though the Cretaceous limestone forms its basement, the Pliocene-Pleistocene lahar is the dominant lithology in the watershed, with up to 30 m thick tabular and cross laminations of volcanic ash and andesitic rock fragments (Fries, 1960; Arce et al., 2013). The other dominant lithology of the watershed is Oligocene rhyolite, exposed at the southwestern margin of the basin, at about 4 km from the actual water body (Fries, 1960). Thus, the sedimentary deposit of this shallow lacustrine basin is of volcanoclastic origin (Roy et al., 2020).

The modern era hydroclimate of Lake Coatetelco and its surroundings is influenced by monsoonal rainfall and tropical storms. Both are related to the ITCZ over the eastern Pacific warm pool, off the coast of southern Mexico during the summer

and ENSO modulated easterly winds from the Caribbean Sea during the autumn (Magaña, 1999; Magaña et al., 2003). The years of negative precipitation anomalies are caused by El-Niño conditions and the associated displacement of the ITCZ toward southerly latitudes and fewer tropical cyclones over the Intra Americas Seas in the Atlantic Ocean during the autumn (Magaña et al., 2003). Instrumental records comprising four decades between 1957 and 1998 CE indicated < 10/year tropical cyclones over the Intra Americas Seas during the El-Niño years (Magaña et al., 2003). However, the warmer SST (up to 3°C) in the tropical northeast Pacific Ocean increases the potential for hurricanes with more intense winds to last longer during the El-Niño years (De Maria and Kaplan, 1994). Between 1955 and 2016 CE, the meteorological station at Miacatlán (at 4 km north of the lake) recorded annual precipitations of 600–2486 mm (average: 1047 mm), most of it in the summer and autumn months (May–October), and relatively higher annual evaporations of 1354–2616 mm (average: 1844 mm) (Servicio Meteorológico Nacional, CONAGUA, México). The maximum temperatures of 41–42°C occurred between April and June and the minimum temperatures of 3–8°C were registered between November and March. The lake water column was mostly controlled by the droughts in the recent past. For example, the severe droughts of 1928–1930 CE left the lacustrine basin completely dry (Mazari, 1986). The drilling of deep wells for irrigation in the immediate lake vicinity of the lake (e.g., 1989 CE) has also reduced the water column by enhancing erosion in the catchment (Maldonado, 2005). Over the last couple of years, the lake has been retaining a maximum water column of 4–5 m due to the construction of a channel that comes from the Tembembe River (Maldonado, 2005, **Figure 2**). However, the La Angostura Ravine continues to feed the lake both during the summer as well as autumn (Contreras-MacBeath et al., 2004; Maldonado, 2005).

The archeological site of the most important religious-political center of the Xochicalco culture is situated at 8 km from the lake and it emerged as a confederation of towns south of the Chichinautzin volcanic range during the late Classic period (~650–900 CE), after the fall of Teotihuacan (González and Garza, 1994; Hirth, 2000; Webb and Hirth, 2000; Alvarado and Garza, 2010). The arid hydroclimate during its demise has been recently documented (Roy et al., 2020) and this new climate record, apart from the variability over the Holocene, addresses the hydrological conditions during initiation of the archeological history of this region that dates at least to ~3 cal ka BP with the arrival of small groups of the Olmec families from the Gulf of Mexico (Angulo, 1978). The Tlahuicas group occupied the central and western parts and the Xochimilcas group occupied the northern and eastern parts of the current Morelos state (**Figure 2**, Díez, 1933; Angulo, 1978; Smith, 2010). Human influence is represented by permanent sites for religious and ceremonial activities, as well as commercial exchange centers in the vicinity of the Lake Coatepetl and next to the nearby streams during the late Pre-Classic (400 BCE–200 CE) (Angulo, 1978). Settlements were concentrated around the Coatlán Viejo site and on the banks of the Chalma, Amacuzac, and Tembembe rivers (**Figure 2**, Hirth, 2010). The archeological evidence in the western part of the Morelos state, however, was relatively older (1200–400 BCE;

Angulo, 2010). Small settlements at Coatepetl emerged around ~500 BCE without architectural structures (Konieczna, 1992), and the population increased with the most representations at Gualupita, Nexpa, San Pablo, Atlahuacán, Olinitepec, and Chalcatzingo sites of the Tlatilco culture (**Figure 2**, Grove, 2010).

## SEDIMENT CORE AND ANALYSIS

A 750-cm long sediment core (COA-N2-2019) was collected from the seasonally dry southwestern margin of the present-day Lake Coatepetl and the top 50 cm (50–0 cm) was lost during the sample recovery. This study is focused on the geochemical and stable isotope compositions of sediments between 412 and 50 cm depths (ca. 11.5–2.1 cal ka BP, see **Supplementary Table 1** for all data) as the objective was to reconstruct the environmental and hydrological changes that occurred since the earliest Holocene and until the first human occupations in this region (**Figure 3**). Sediment textures were defined after macroscopic inspection in the laboratory and a total of 73 samples of 2-cm thick sediment layers were collected at 5-cm intervals (e.g., 50–52 cm, 55–57 cm, 60–62 cm, etc.) from the core. All the samples were oven-dried at 50°C and grounded using an agate mortar and pestle. The oxides of major elements and concentrations of trace elements were measured in a traditional Rigaku Primus II SRS 3000 wavelength dispersive X-ray fluorescence (XRF) spectrometer at Universidad Nacional Autónoma de México. We transformed the oxides into elements by using the element atomic mass/oxide molecular mass ratios. Chronology of the sedimentary sequence is based on AMS <sup>14</sup>C analysis (International Chemical Analysis Inc., Sunrise, FL, United States) of bulk organic matter after removing all the carbonates from eight different sediments sampled at 68–70, 92–94, 130–132, 173–175, 218–220, 371–373, 382–385, and 410–412 cm depths. All of them were calibrated to cal yr BP/cal ka BP using the IntCal20 database in OxCal 4.4 (Reimer et al., 2020).

The concentrations of total carbon (TC) and total nitrogen (TN) were estimated in a 50-position automated Zero Blank sample carousel of ECS 8020 elemental analyzer at the University of Florida. After the flash combustion of samples in a quartz column containing chromium oxide and silvered cobaltous/cobaltic oxide at 1000°C in an oxygen-rich atmosphere, the sample gases were transported in a He carrier stream and passed through a hot reduction column (650°C) consisting of reduced elemental copper to remove oxygen. The water vapor was removed by passing the effluent stream through a chemical (magnesium perchlorate) trap and subsequently, both the N<sub>2</sub> and CO<sub>2</sub> gases were separated by passing the stream through a 1.5-m GC column at 55°C. A thermal conductivity detector measured the size of pulses of both the gases. For the total inorganic carbon (TIC) analysis, the samples were acidified with 1N phosphoric acid, and the evolved CO<sub>2</sub> was measured coulometrically using a UIC (Coulometrics) 5017 CO<sub>2</sub> coulometer coupled with an AutoMate automated carbonate preparation device<sup>1</sup>. Approximately 15 mg of sample was weighed into septum top tubes and placed into the AutoMate

<sup>1</sup><http://www.automatefx.com/>

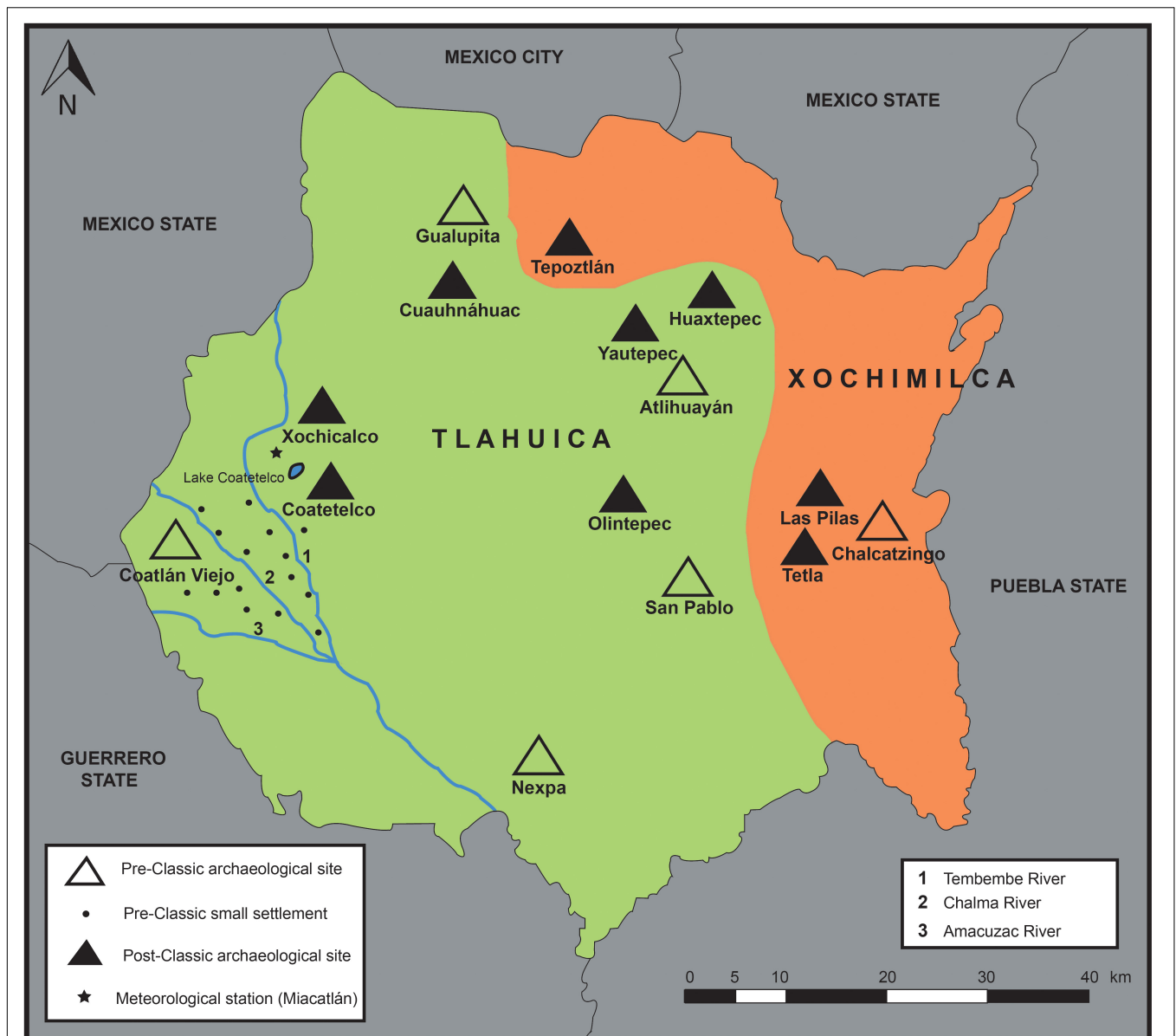


**FIGURE 2 |** Map showing the locations of settlements since the Pre-Classical period of Mesoamerica in vicinity of the Lake Coatetelco and banks of important rivers in the region. Coatetelco had small settlements since ~500 BCE and it remained as an important regional center until its conquest by the Mexica during ~1430 CE. Xochicalco was a confederation of towns during the late Classical period (650–900 CE).

carousel and the system software monitors the  $\text{CO}_2$  measurement until the evolved  $\text{CO}_2$  plateaus. Total organic carbon (TOC) was calculated by subtracting TIC from TC. As calcite was the only carbonate mineral in the samples (see section “Mineralogy and Chronology of COA-N2-2019”), TIC was expressed here as  $\text{CaCO}_3$  using the equation:  $\text{CaCO}_3 (\%) = \text{TIC} (\%) \times 8.33$ , where 8.33 is the ratio of the molecular weight of calcite ( $\text{CaCO}_3$ ) and atomic weight of Ca. Stable isotopes of carbon in organic matter ( $\delta^{13}\text{C}_{\text{org}}$ ) were measured after acidifying the samples with 1N hydrochloric acid overnight in 15 ml centrifuge tubes to remove the carbonates. This procedure includes decanting of the acid and subsequent addition of new acid and stirring up the sample

using a vortex mixer. Two identical rinses involve addition of deionized water, stirring up of the samples, and then removal of water. Acidified material is combusted in a Carlo Erba NA1500 CNS elemental analyzer at  $1000^\circ\text{C}$ , and the resultant  $\text{CO}_2$  was passed to a ConFlo II interface and into the inlet of a Thermo Electron Delta V Advantage isotope ratio mass spectrometer running in continuous flow mode at the University of Florida.  $\delta^{13}\text{C}_{\text{org}}$  values were measured with the precision of 0.03–0.06‰ and are reported in permil (‰) relative to the VPDB (Vienna Pee Dee Belemnite). Clastic and non-clastic minerals were identified in all the samples using SIEMENS D5000 X-ray diffractometer at Universidad Nacional Autónoma de México. Thin sections

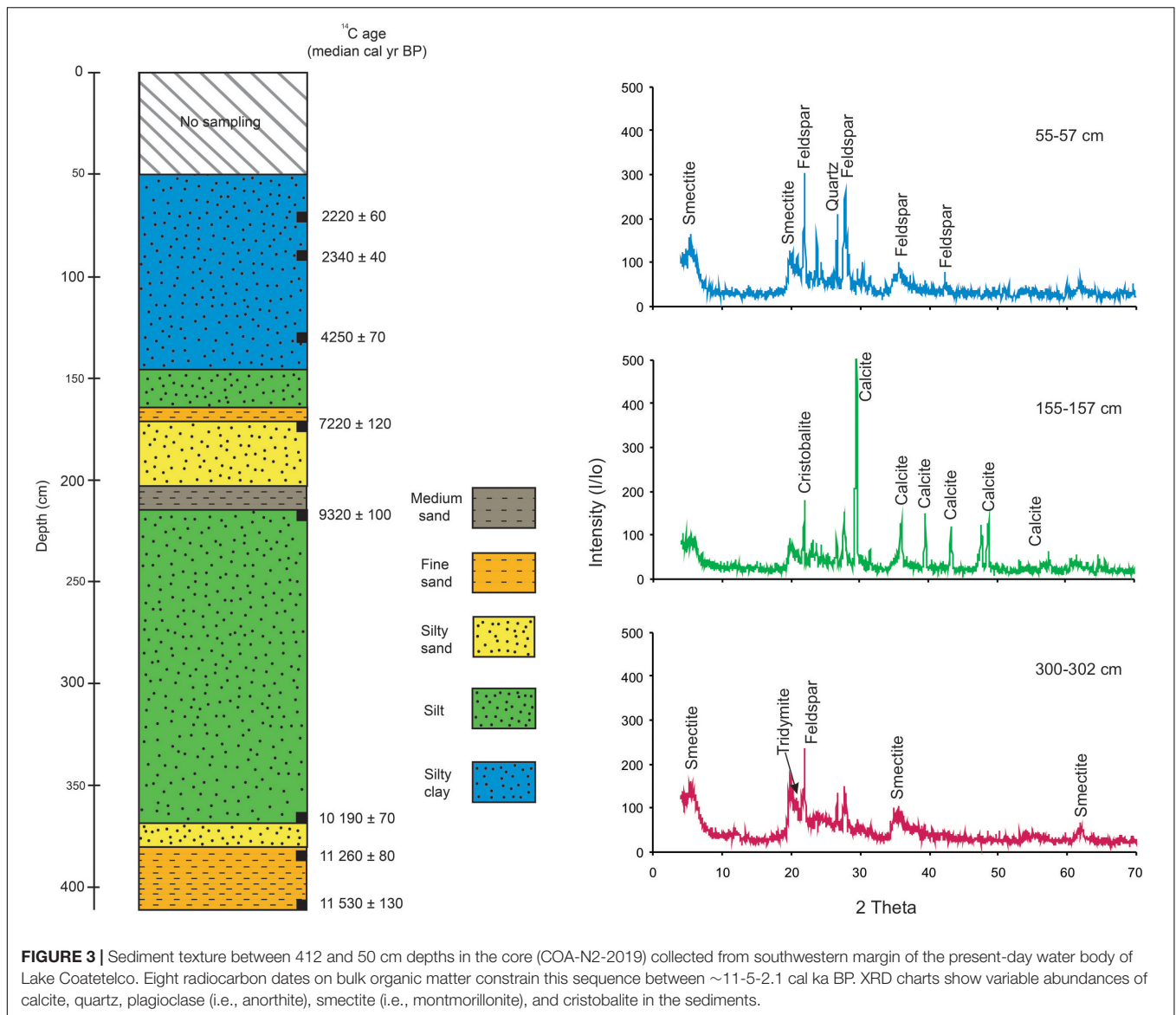


**FIGURE 3 |** Sediment texture between 412 and 50 cm depths in the core (COA-N2-2019) collected from southwestern margin of the present-day water body of Lake Coatetelco. Eight radiocarbon dates on bulk organic matter constrain this sequence between ~11-5-2.1 cal ka BP. XRD charts show variable abundances of calcite, quartz, plagioclase (i.e., anorthite), smectite (i.e., montmorillonite), and cristobalite in the sediments.

were prepared from a total of six different unconsolidated sediments at intervals with minimal and abundant calcite by following Camuti and McGuire (1999). Chemical weathering of silicates was quantified by estimating the chemical index of alteration (CIA) and plagioclase index of alteration (PIA), using the molar concentrations of Al, Ca, Na, K, and P oxides in siliclastic fractions as well as CO<sub>2</sub> present in carbonates (e.g., Nesbitt and Young, 1984, 1989; Fedo et al., 1995; Roy et al., 2008). Due to the presence of calcite and possible apatite in sediments, the CaO content in silicate fractions (CaO\*) was calculated after correcting the bulk sediment CaO for carbonate and phosphate contents as:  $CaO^* = CaO - CO_2 - (10/3) \times P_2O_5$  (Fedo et al., 1995). A total of 12 lake water samples representing four different seasons of 2021 CE (spring, summer, autumn, and winter) were collected and measured for total dissolved solids (TDS) and Hydrogen ion concentration (pH) using a Hanna instrument (HI98130). Concentrations of cations and

anions were determined in the Waters corporation liquid chromatograph. Water-minerals saturation index (SI) for calcite was estimated in PHREEQC v.3.0 using the formula,  $SI = \log(IAP/KT)$ , where SI is the saturation index, IAP is the ion activity product of the mineral, and KT is the equilibrium constant (Parkhurst and Appelo, 2013).

## RESULTS

### Mineralogy and Chronology of COA-N2-2019

This sedimentary register lacks primary structures and desiccation fissures, and it is composed of medium-bedded to thick-bedded light brown fine sand between 412 and 385 cm, light brown silty-sand between 385 and 373 cm, silt with different tones of brown and gray between 373 and 218 cm,

brown medium sand between 218 and 207 cm, brown silty-sand between 207 and 175 cm, a layer of brown fine sand between 175 and 168 cm, brown silt between 168 and 150 cm, and dark gray silty-clay between 150 and 50 cm depths (**Figure 3**). The contacts of all the sedimentary units with underlying and overlying units are transitional, except for the sharp contact between the fine sand layer at 175–168 cm and the overlying silt layer at 168–150 cm. This sharp contact at 168 cm might be due to disruption in sediment accumulation, and a possible depositional hiatus during the low lake low stands at the coring site. Organic matter (mostly root remnants) is visible in the silty clay of 70–50 cm. Similarly, the volcanic rock fragments (occasionally up to 2 cm) are observed in sediments of 168–50 cm depth (**Figure 3**). XRD charts show variable abundances of calcite ( $\text{CaCO}_3$ ), quartz, plagioclase (i.e., anorthite), smectite (i.e., montmorillonite), and cristobalite (**Figure 3**). Only the sediments of 157–100 cm depths have abundant calcite and the rest of the samples either lack or have traces of calcite. Calcite in thin sections represents massive micrite without internal structures along with clastic matrix composed of quartz and feldspars. The clastic matrix is minimal in sediments of 157–100 cm.

An age-depth model constructed from calibrated  $^{14}\text{C}$  ages of the bulk organic carbon in sediments using OxCal version 4.4 (P sequence,  $k = 0.05$ ) constrains the geochronology of this sediment record (Bronk Ramsey, 2008, 2009; Bronk Ramsey and Lee, 2013; Reimer et al., 2020). **Table 1** presents the radiocarbon ages,  $\delta^{13}\text{C}_{\text{org}}$ , modeled calibrated ranges ( $2\sigma$ ) and corresponding median values. This Bayesian age model with uncertainties of 40–130 years assigned chronology to the sediment layers analyzed for mineralogy and geochemistry (**Figure 4**). Agreement indices (A) of the radiocarbon ages varied between 82.5 and 121.4% and the age model has an agreement index of 112.2%. Considering the depositional rates of 0.02–0.35 cm/yr, each sample represented the average of depositional histories between ~10 and 270 cal yr and the age differences of two consecutive samples were ~25–430 cal yr (sub-millennial-scale). Radiocarbon analysis of organic matter at 410–412 cm depth assigned a median age of ~11.5 cal ka BP to the base of this sediment record and the extrapolation of calibrated  $^{14}\text{C}$  values indicated depositional age of ~2.1 cal ka BP for the core top (50–52 cm depth).

The fine sand layers at 412–385 and 175–168 cm depth were deposited during ~11.5–11.2 and at ~7 cal ka BP, respectively. Similarly, the medium sand layer at 218–207 cm depth was deposited at ~9 cal ka BP and the massive silt at 373–218 cm depth represented the depositional history between ~10.5–8 cal ka BP. Lower depositional rates (i.e., 14.5 and 11.7 cm/ka, **Figure 4**) might be representing a possible hiatus or poor sediment preservation between ~7.2 and 4.2 cal ka BP (middle Holocene) and another depositional hiatus between ~11.2 and 10.2 cal ka BP (early Holocene). The early Holocene sediments with a possible hiatus were represented by silty sand, whereas the middle Holocene sediments were represented by a sharp contact between fine sand and silt layers (**Figure 3**). Although the catchment lithologies are represented by volcanic deposits of both mafic and felsic compositions, the dissolved old carbon from the basement limestone in bulk organic matter might have caused offset in ages. We evaluated the chronologies of sub-millennial-scale paleohydrological changes by comparing the new registers with other records from southwestern and western Mexico (see section “Paleohydrology” and **Figure 5**).

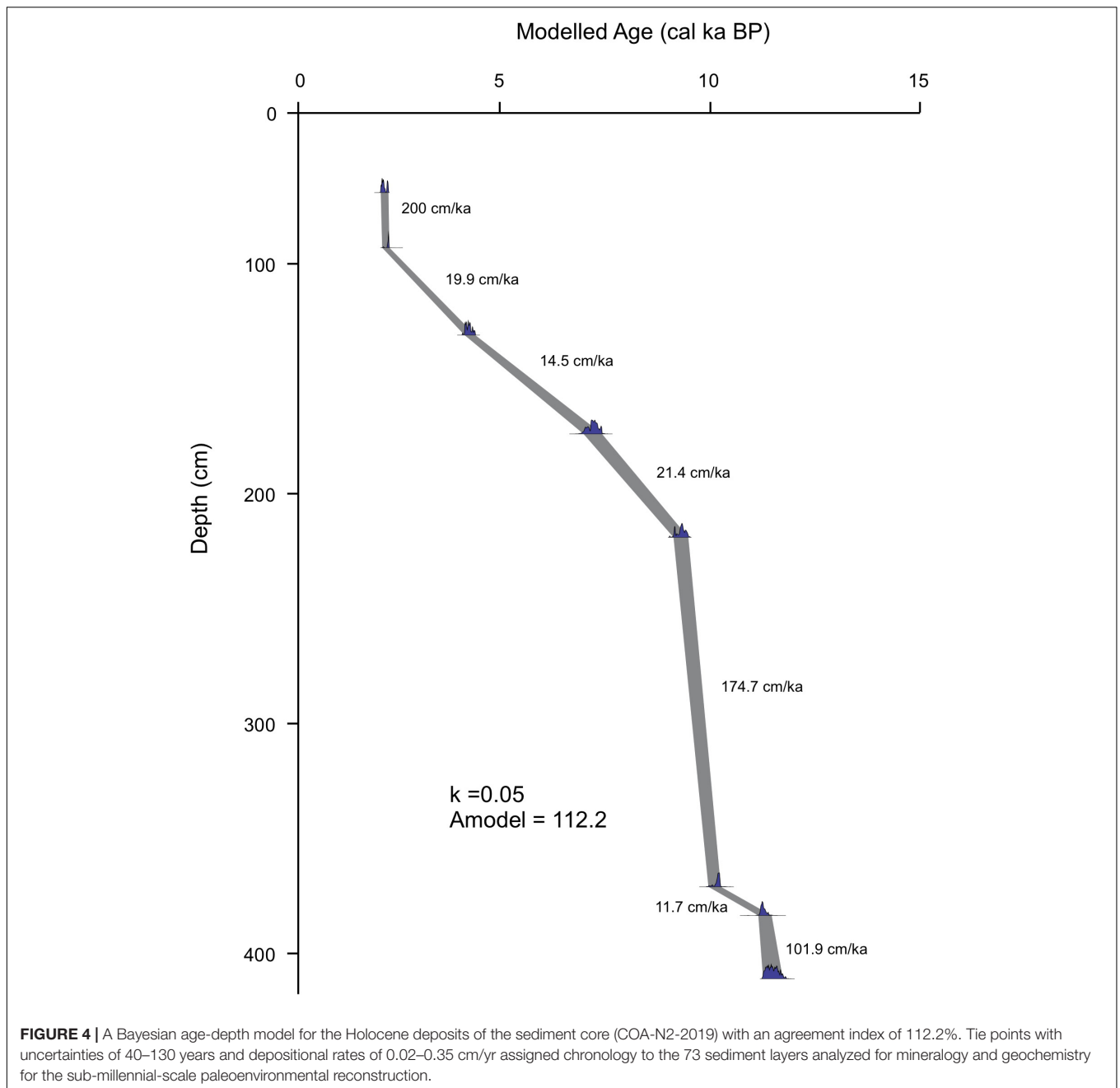
### Total Organic Carbon, C/N, and Carbon Isotopes ( $\delta^{13}\text{C}_{\text{org}}$ )

Total organic carbon (0.09–0.81%; average: 0.38%) reflects the abundance of preserved organic matter (**Figure 6**). Sediments deposited during ~10–9.5 cal ka BP, at ~6 cal ka BP and again during ~4.2–2.1 cal ka BP have above-average values and the rest of the sediments have below-average TOC (<0.38%). TN content varies between 0.02 and 0.07% with an average of 0.04%. C/N ratio (3–28; average: 10.7) is positively correlated ( $r = 0.7$ ,  $p > 0.05$ ) with TOC and it generally remains < 20, except for the sample representing ~6 cal ka BP with C/N of >20 (**Figure 6**). Sediments of ~6–2.1 cal ka BP show above-average values with C/N generally remaining between 10 and 20. With some minor variations (e.g., ~10 cal ka BP), C/N mostly remains < 10 in the sediments of ~11.5–6 cal ka BP. The carbon isotope compositions ( $\delta^{13}\text{C}_{\text{org}}$ ) of bulk organic matter vary between –25.36 and –15.53‰ VPDB with an average of –20.01‰ VPDB (**Figure 6**). It shows moderate positive correlations with C/N ( $r = 0.6$ ,  $p < 0.05$ ) and TOC ( $r = 0.7$ ,  $p < 0.05$ ).

**TABLE 1** | Radiocarbon analysis of bulk organic matter in sediments, calibrated results, and modeled ages used for the Bayesian age-depth model of a core from southwestern margin of Lake Coatetelco (central Mesoamerica) in OxCal version 4.4 (P sequence,  $k = 0.05$  and  $A_{\text{model}} = 112.2$ ).

Depth (cm)	Lab. code	AMS $^{14}\text{C}$ age (BP)	$2\sigma$ range (cal yr BP)	Modeled median probability (cal yr BP)	Agreement index (A)	$\delta^{13}\text{C}_{\text{org}}$ (‰) V-PDB
68–70	19OS/1057	2260 ± 30	2150–2340	2220 ± 60	96.9	–15.9
92–94	14C-5464	2300 ± 30	2180–2360	2340 ± 40	121.4	–16.0
130–132	14C-5465	3840 ± 30	4140–4410	4250 ± 70	99.5	–17.2
173–175	19OS/1058	6310 ± 100	6980–7430	7220 ± 120	99.8	–20.9
218–220	14C-5837	8370 ± 60	9130–9490	9320 ± 100	82.5	–22.5
371–373	14C-5838	8990 ± 60	9960–10260	10190 ± 70	120.4	–23.5
382–385	19OS/1059	9860 ± 70	11,160–11,500	11,260 ± 80	114	–24.0
410–412	14C-5467	9980 ± 70	11,260–11,740	11,530 ± 130	100.9	–25.4

Carbon isotope compositions ( $\delta^{13}\text{C}_{\text{org}}$ ) of bulk organic carbon varied between –25.4 and –15.9 ‰ VPDB.

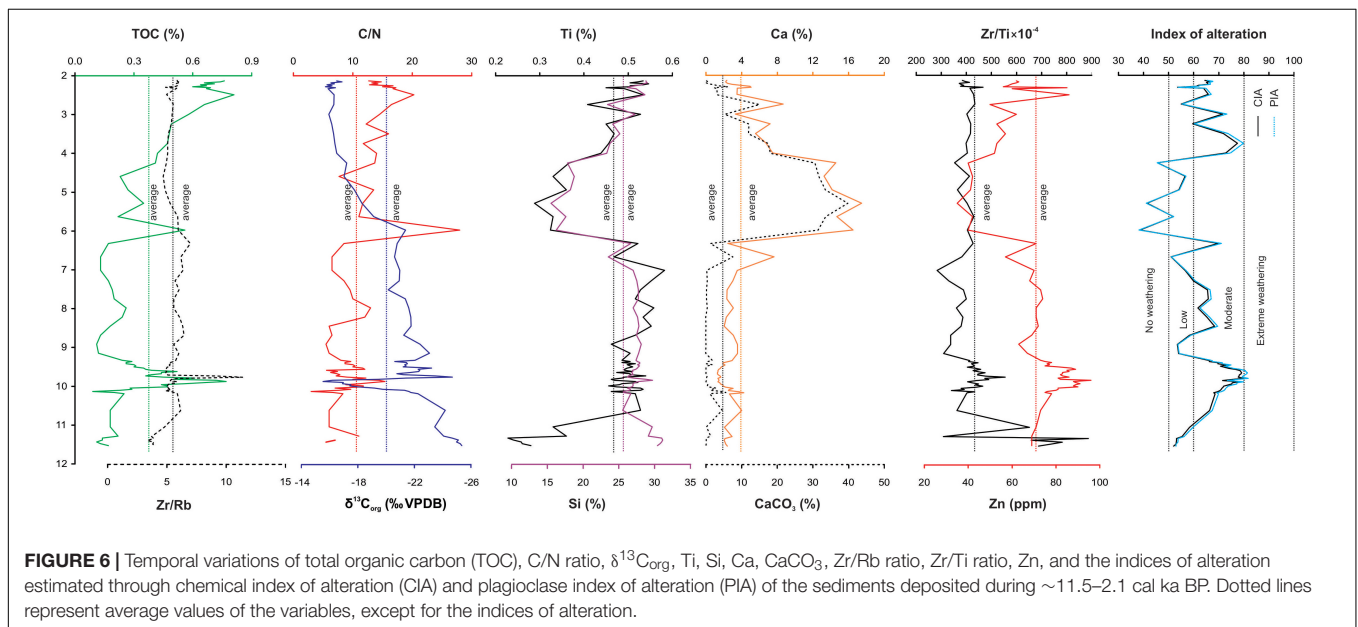
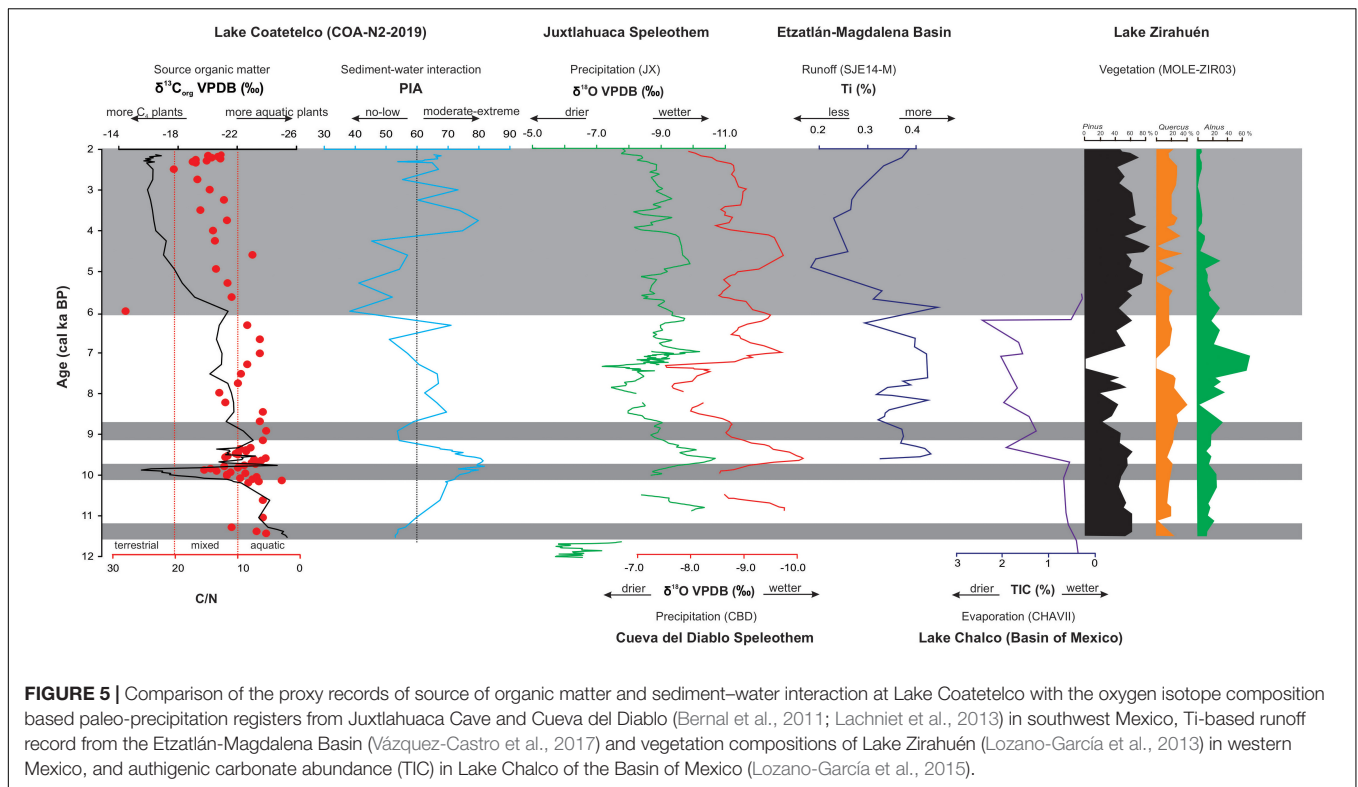


Above-average values of  $\delta^{13}\text{C}_{\text{org}}$  represent the sediments of  $\sim 10$  and  $\sim 5.6$ – $2.1$  cal ka BP. Sediments deposited between  $\sim 4.2$  and  $2.1$  cal ka BP have homogeneous and more-than-average values ( $-17.21$  to  $-15.80\%$  VPDB).

### Multi-Elements and $\text{CaCO}_3$

Stratigraphic distributions of Ti (0.23–0.81%; average: 0.47%), Al (2.91–5.84%; average: 4.63%), Fe (1.05–2.36%; average: 1.83%), and Mg (0.55–1.98%; average: 1.14%) are similar ( $r = 0.6$ – $0.8$ ,  $p < 0.05$ ) as they represent the abundances of clastic minerals. The distribution of Si (15.51–31.13%; average: 26.53%) is slightly different with an absence of any significant correlation with Ti

( $r = 0.2$ ,  $p < 0.05$ ). Both Ca (1.29–17.46%; average: 3.87%) and Na (0.27–1.45%; average: 0.62%) are inversely correlated ( $r = -0.4$  to  $0.5$ ,  $p > 0.05$ ) and K (0–0.05%; average: 0.03%) lacks correlation ( $r = -0.1$ ,  $p < 0.05$ ) with Ti. The content of  $P$  varies between 0–0.4% with an average of 0.02%. **Figure 6** shows the abundances of Ti, Si, and Ca as representative elements with different temporal distributions. Both Ti and Si have above-average values in sediments deposited during  $\sim 10.2$ – $6$  cal ka BP and average to below-average values in sediments of  $\sim 6$ – $3.2$  cal ka BP. Both have fluctuating contents in sediments representing  $\sim 3.2$ – $2.1$  cal ka BP. Sediments of  $\sim 11.5$ – $10.2$  cal ka BP have above average Si and below-average Ti. All these elements, except



for Ca, represent abundances of clastic minerals, both silicates and clay minerals, eroded from watershed into the lacustrine basin. However, the distribution of Ca is similar ( $r = 0.9, p < 0.05$ ) to  $\text{CaCO}_3$  (0–39.73%; average: 4.70%). Above-average values of both during  $\sim 6$ – $3.2$  cal ka BP represent the sediments with higher calcite abundance and average to below-average values during  $\sim 11.5$ – $6$  cal ka BP represent the sediments with lower calcite precipitation (Figure 6). Both have fluctuating contents in

sediments of  $\sim 3.2$ – $2.1$  cal ka BP. Ca of 1.29–3.54% in sediments lacking any  $\text{CaCO}_3$  (e.g.,  $\sim 10$ – $7$  cal ka BP) reflects that a part of it is associated with plagioclase (i.e., anorthite). The abundance of  $\text{CaCO}_3$  lacks correlation with TOC ( $r = 0.01, p > 0.05$ ) and the distributions of  $\text{CaCO}_3$  and  $\text{CaCO}_3/\text{Ti}$  are similar ( $r = 0.98, p > 0.05$ ).

Distributions of Zr (111–273 ppm; average: 197 ppm), Cu (21–52 ppm; average: 36 ppm) and Zn (35–96 ppm; average:

71 ppm) are similar ( $r = 0.7$ ,  $p < 0.05$ ), and they are represented by temporal variations of Zn in **Figure 6**. The distribution of Rb (22–52 ppm; average: 37 ppm) is slightly different with moderate correlation with Zr ( $r = 0.6$ ,  $p < 0.05$ ). The Zr/Rb ratio varies between 3.4 and 11.4 (average: 5.5; **Figure 6**) and the minimal influence of the grain size on this ratio is reflected by its lower values in the fine sand layers of 412–385 cm (~11.5–11.2 cal ka BP; Zr/Rb: 3.4–4.0) and 175–168 cm (~7 cal ka BP; Zr/Rb: 6.1–6.4) compared to the silt of 287–298 cm (~10 cal ka BP; Zr/Rb: 9.2–11.4). All the trace elements, except for Rb, show below-average values in sediments of ~11.5–11.2 cal ka BP. Sr (210–608 ppm; average: 367 ppm) shows inverse correlation ( $r = -0.8$ ,  $p > 0.05$ ) with Zn and its distribution is comparable to  $\text{CaCO}_3$  ( $r = 0.5$ ,  $p < 0.05$ ). Positive correlation between Zr and Ti ( $r = 0.5$ ,  $p < 0.05$ ) is indicative of the similar distributions of both Zr-bearing and Ti-bearing clastic minerals. However, Zr/Ti ratio is variable ( $284\text{--}886 \times 10^{-4}$ ; average:  $435 \times 10^{-4}$ ) and its higher values represent the fine-sand layer of ~11.5–11.2 cal ka BP with above-average Rb (**Figure 6**).

## Chemical Weathering

Climate plays a dominant role in regulating the chemical weathering of sediments and rocks present in the catchment and Shao et al. (2012) observed synchronous increases in values of chemical index of alteration (CIA) with climate parameters, such as precipitation, temperature, and runoff in China. CIA as well as the values of plagioclase index of alteration (PIA) estimated the different degrees of chemical weathering of silicate minerals (**Figure 6**). CIA ( $=[\text{Al}_2\text{O}_3/(\text{Al}_2\text{O}_3 + \text{CaO}^* + \text{Na}_2\text{O} + \text{K}_2\text{O})] \times 100$ ) appraised chemical alteration of feldspars to clay minerals through sediment-water interaction during the transportation from watershed (e.g., Nesbitt and Young, 1984; Roy et al., 2008, 2012). Similarly, PIA ( $=[(\text{Al}_2\text{O}_3 - \text{K}_2\text{O})/(\text{Al}_2\text{O}_3 + \text{CaO}^* + \text{Na}_2\text{O} - \text{K}_2\text{O})] \times 100$ ) estimated the transformation of plagioclase to clay minerals through chemical alteration during the transportation (e.g., Fedo et al., 1995; Roy et al., 2008, 2012). Both the indices with values  $\leq 50$  represent the sediments lacking any chemical weathering. Sediments with low weathering, moderate weathering, and extreme weathering are represented by values of 50–60, 60–80, and  $>80$ , respectively (Fedo et al., 1995). The indices show comparable values ( $r = 0.99$ ,  $p < 0.05$ ) in sediments with CIA varying between 39 and 80 (average: 66) and PIA between 38 and 82 (average: 67) (**Figure 6**). They are positively correlated with Ti ( $r = 0.6$ ,  $p < 0.05$ ) and negatively correlated with  $\text{CaCO}_3$  ( $r = -0.6$ ,  $p < 0.05$ ), suggesting more previously weathered materials were delivered into the lake along with Ti-enriched sediments and less previously weathered materials were delivered along with Ti-depleted sediments and more  $\text{CaCO}_3$  precipitated. The sediments deposited during ~11.5–11.2 cal ka BP also contained siliciclastic minerals characterized by low chemical alteration. The sediments of ~10.2–6 cal ka BP are characterized by generally moderate CIA values and moderate-to-extreme PIA values. However, the sediments deposited during ~6–4.2 cal ka BP contain siliciclastic minerals characterized by a lack of weathering to low weathering. The sediments of ~4.2–2.1 cal ka BP have

generally moderately weathered siliciclastic fractions with fluctuations.

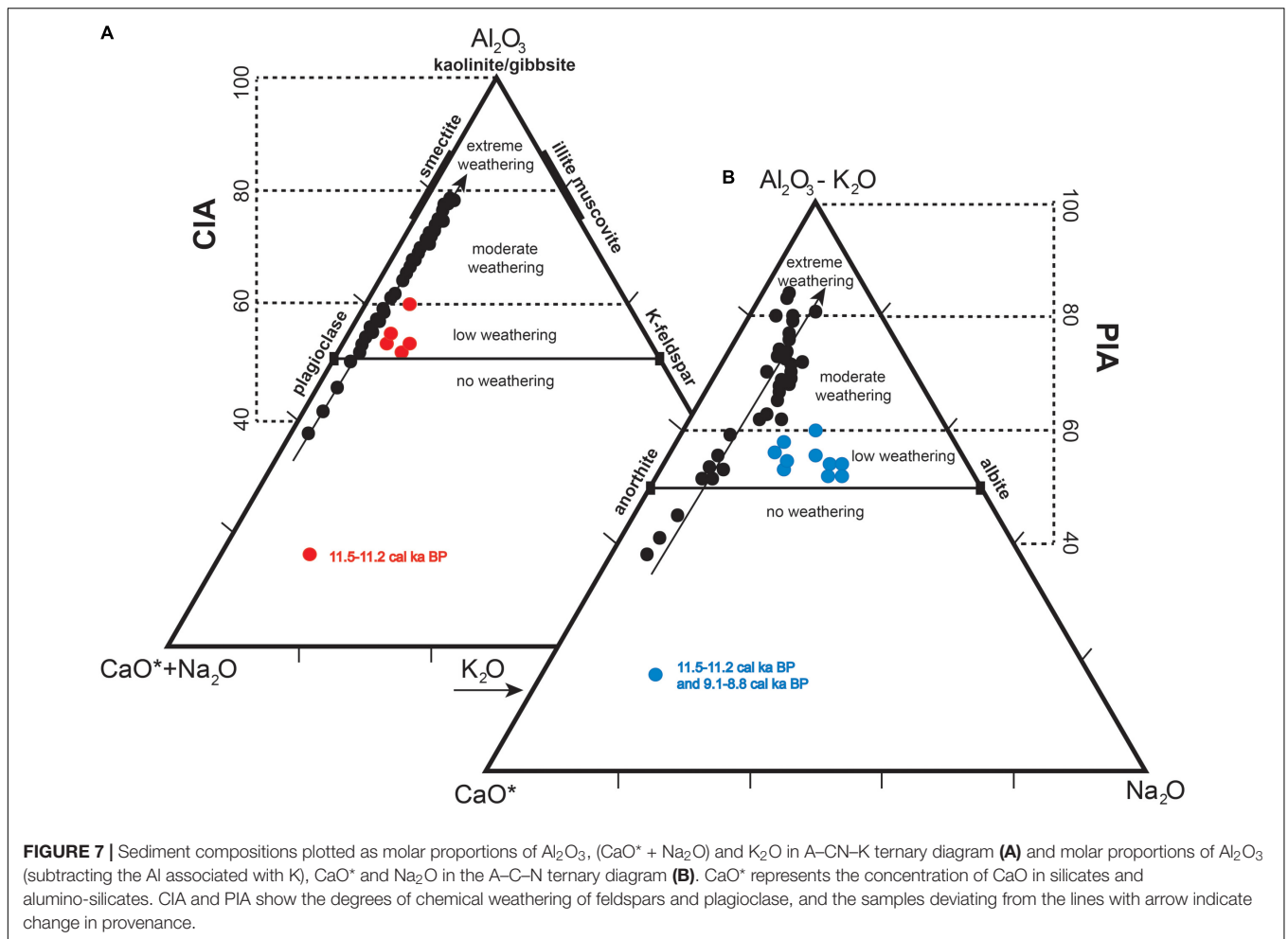
## Ternary Diagrams and Sediment Provenance

Molar proportions of  $\text{Al}_2\text{O}_3$  (A),  $\text{CaO}^* + \text{Na}_2\text{O}$  (CN), and  $\text{K}_2\text{O}$  (K) in siliciclastic fractions were plotted in A-CN-K ternary plot, while the molar proportions of  $\text{Al}_2\text{O}_3\text{-K}_2\text{O}$  (A),  $\text{CaO}^*$  (C) and  $\text{Na}_2\text{O}$  (N) were plotted in A-C-N ternary plot to evaluate the source materials as the clastic components have variable Zr/Ti ratios (**Figure 7**). In A-CN-K ternary plot, most of the samples fall along a linear trend showing different degrees of chemical weathering. Intersection of this trend with the feldspar join indicates a provenance with abundant plagioclase and minimal K-feldspars, comparable to the andesitic lahars, dominant in the immediate vicinity. The sediments with low chemical weathering deposited during ~11.5–11.2 cal ka BP deviate slightly from this linear trend (marked as red circles) showing relatively more K-feldspar compared to the andesite lahar in the provenance (**Figure 7A**). Distribution of sediments in the A-C-N ternary space indicates that the source rock for most of the deposits has abundant anorthite. Deviation of the sediments deposited during ~11.5–11.2 cal ka BP and ~9.1–8.8 cal ka BP (marked as blue circles), however, indicates a felsic source with relatively more albite (**Figure 7B**).

## DISCUSSION

### Paleohydrology

The geochemical proxies of erosion, chemical alteration of deposited sediments, and water column salinity reconstructed the paleohydrological conditions of Lake Coatetelco in central Mesoamerica (**Figure 8**). The immobility in environments of variable pH and Eh makes titanium (Ti) an ideal proxy for reflecting detrital material abundance through erosion in the watershed. However, it is affected by provenance of the clastic sediments and the lower values could also reflect the intervals of higher erosion from felsic rocks in the watershed. Both CIA and PIA are unaffected by change in the sediment provenance, and they indicate chemical alterations of feldspars (i.e., plagioclase) to clay minerals (i.e., smectite) through sediment-water interaction in the watershed. Different proportions of plagioclase/K-feldspars and albite/anorthite inferred in the A-CN-K and A-C-N ternary spaces suggested change in the mineralogical assemblage of sediments deposited during ~11.5–11.2 cal ka BP and ~9.1–8.8 cal ka BP, reflecting a different sediment provenance than the rest of the record (**Figure 7**). Above-average values of Zr/Ti and Rb in these sediments suggested more Zr-bearing mineral deposition from relatively felsic rocks (**Figure 6**). The CIA/PIA indices are generally consistent with increased delivery of catchment materials between ~10.2 and 6 cal ka BP and the reduced delivery between ~6 and 4 cal ka BP. However, the higher and lower sediment-water interactions did not emphasize centennial timescale hydroclimate changes. The moderate-to-extreme alterations (CIA and PIA  $\geq 60$ ) along with deposition



of above-average Ti-bearing sediments represented the intervals of more erosion in the watershed and the transportation of weathered sediments dominantly via runoff. Similarly, the lack-to-low alterations (CIA and PIA < 60) along with the deposition of below-average Ti-bearing sediments represented the intervals of transportation of sediments with minimal or absence of any chemical alteration into the basin under water-scarce conditions with minimal runoff. As the indices of chemical alterations are unaffected by geology and the degrees of chemical weathering have established ranges, we compared the CIA values of this study with Shao et al. (2012) that reported CIA of 70–80 for the fine-grained surface sediments from 13 major rivers in China with catchments receiving mean annual precipitation comparable to Lake Coatetelco. Even within the range of moderate weathering, the CIA increased with warmer temperature and higher precipitation in the catchments suggesting enhanced weathering intensity in warm and humid environments. Abundances of Ti, complemented by PIA values, are considered here as a proxy to demarcate wetter intervals and periods of more runoff. The PIA-enriched sediments were deposited during the intervals of more runoff and more precipitation.

In this basin with dominant volcanic and volcanoclastic deposits, the  $CaCO_3$ -enriched sediments could reflect the influence of photosynthesis of aquatic plants and subsequent  $CO_2$  degassing and/or loss of  $CO_2$  through evaporation (Cohen, 2003). Lack of any correlation between  $CaCO_3$  and TOC ( $r = 0.01$ ,  $p > 0.05$ ) suggests minimal influence of organic productivity (e.g., photosynthesis of aquatic plants) on calcite precipitation. The relatively higher saturation index of calcite in lake water of higher salinity (TDS) suggests supersaturation and more calcite precipitation from more saline water column and evaporative conditions. Hence, the above-average  $CaCO_3$  values are considered as a proxy to represent the intervals of more saline water and generally evaporative conditions. Our proxy interpretation is similar to the records of Lake Chalco in the Basin of Mexico (Lozano-García et al., 2015) and the Etzatlán-Magdalena Basin in western Mexico (Vázquez-Castro et al., 2017), both with volcanoclastic geology. The calcite precipitation in Lake Coatetelco was not biologically mediated through the autochthonous productivity. The similar distributions of  $CaCO_3$  and  $CaCO_3/Ti$  ( $r = 0.98$ ;  $p < 0.05$ ) suggest lack of any dilution effect on  $CaCO_3$  abundance from the inputs of clastic minerals from the catchment.

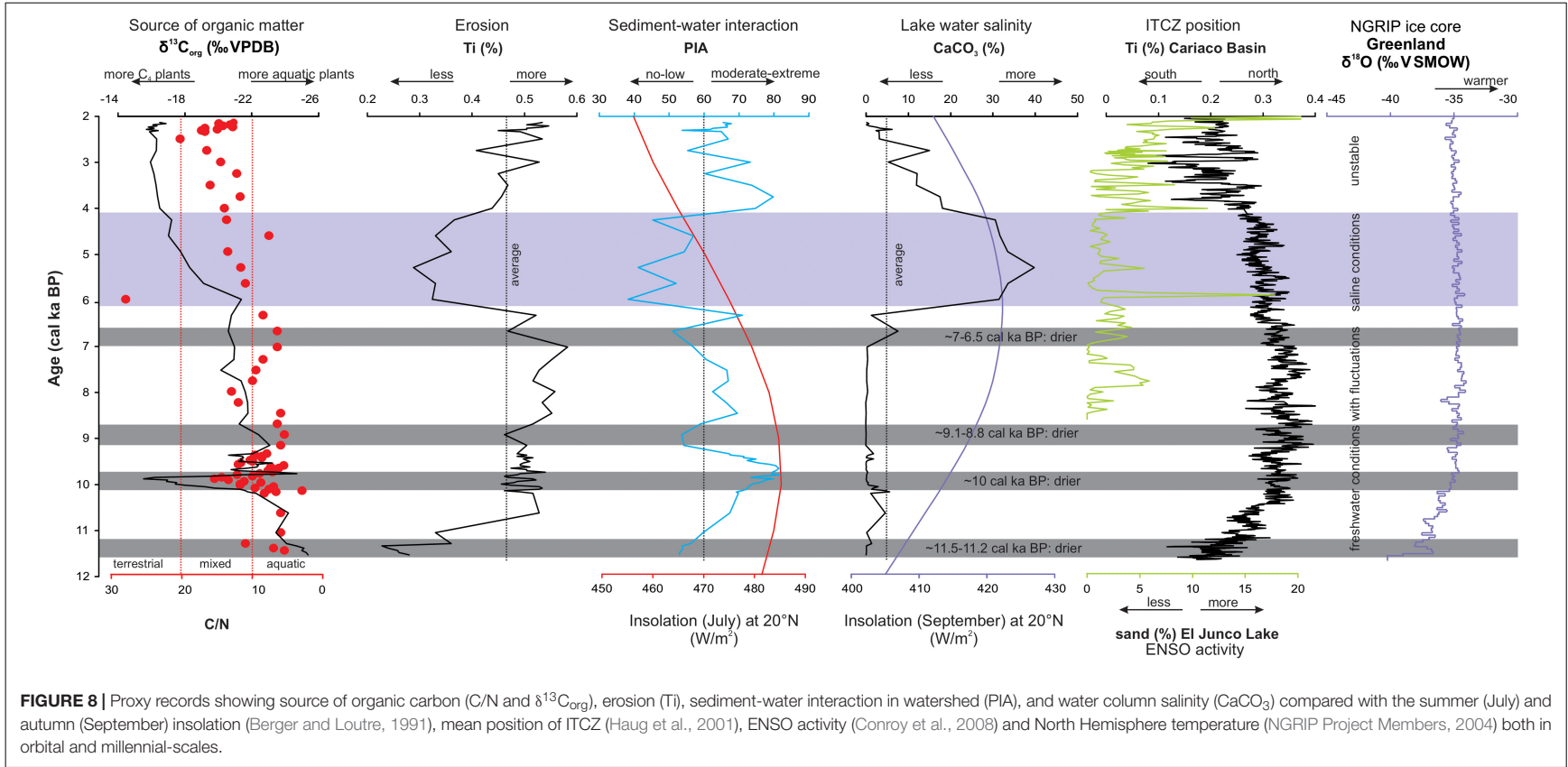


**FIGURE 8 |** Proxy records showing source of organic carbon (C/N and  $\delta^{13}C_{org}$ ), erosion (Ti), sediment-water interaction in watershed (PIA), and water column salinity ( $CaCO_3$ ) compared with the summer (July) and autumn (September) insolation (Berger and Loutre, 1991), mean position of ITCZ (Haug et al., 2001), ENSO activity (Conroy et al., 2008) and North Hemisphere temperature (NGRIP Project Members, 2004) both in orbital and millennial-scales.

Our age model and sampling resolution for the geochemical analysis limited the reconstruction of paleohydrological changes in the millennial-to-multimillennial-scale between  $\sim 11.5$  and 6 cal ka BP and between  $\sim 6$  and 2.1 cal ka BP. The effect of old carbon dissolved from the basement limestone on radiocarbon analysis of bulk organic matter possibly remained minimal and did not alter the chronology of the millennial-scale paleohydrological conditions. Comparison of our register with U/Th based chronologies of paleo-precipitation obtained in speleothems from the Juxtlahuaca Cave and Cueva del Diablo in southwestern Mexico and  $^{14}\text{C}$ -based chronology of runoff dynamics estimated from Ti concentrations in lacustrine deposits of the Etzatlán-Magdalena Basin in western Mexico suggests almost synchronous changes (Bernal et al., 2011; Lachniet et al., 2013; Vázquez-Castro et al., 2017, **Figure 5**). The possible hiatus between  $\sim 11.2$ –10.2 cal ka BP in Lake Coatetelco was contemporary to an event of calcite deposition disruption in both speleothems at  $\sim 10.3$  ka. Similarly, the commencement of the interval representing a reduction in erosion/runoff into Lake Coatetelco at  $\sim 6$  cal ka BP occurred simultaneously as the precipitation at Juxtlahuaca and Cueva del Diablo decreased and runoff into the Etzatlán-Magdalena Basin was reduced (**Figure 5**). The combination of different paleo-hydrological proxies has the advantage of reconstructing both the event-scale processes as well as the average of sedimentary processes that might have occurred in millennial-to-multimillennial scales. Some of the proxies such as Ti and  $\text{CaCO}_3$  possibly reflected the event scale processes. However, the chemical weathering indices recorded both the event-scale processes (synchronous changes in Ti and PIA) as well as an average of a larger interval when the sediments with different degrees of chemical alteration were reworked from the watershed during the events of high runoff (asynchronous Ti and PIA).

#### **$\sim 11.5$ –6 cal ka BP**

Below-average water column salinity ( $\text{CaCO}_3$ ) represented the presence of a generally freshwater column. The degree of chemical alteration of feldspars in the deposited sediments, however, varied (**Figure 8**). Low PIA values of sediments with more K-feldspar and albite reflect the change of source to more rhyolitic lithology at  $\sim 11.5$ –11.2 cal ka BP, constrained with two radiocarbon dates. Rhyolite is the only felsic rock exposed at southwestern margin of the lake, at about 4 km from the coring site (Fries, 1960). The mafic andesitic lahar deposits might also have some felsic ash layers as well. Perhaps, the delivery of chemically altered catchment sediments was also reduced due to reduced runoff. Transportation of mostly fine sand from felsic provenance might be due to the aeolian activity. Deposition of more Zr and Rb-bearing minerals also supported the change in provenance, and the influence of grain size was ruled out using the Zr/Rb ratio (**Figure 6**). Dry conditions possibly continued until  $\sim 10.2$  cal ka BP as the lower depositional rate (11.7 cm/ka) could represent a hiatus between  $\sim 11.2$  and 10.2 cal ka BP, concurrent with the growth interruption in stalagmites from Juxtlahuaca Cave and Cueva del Diablo, and lower water level in Lake Pátzcuaro (**Figure 1**, Bradbury, 2000; Bernal et al., 2011; Lachniet et al., 2013).

Higher Ti and more chemically altered materials likely reflect initiation of a lacustrine phase between  $\sim 10.2$  and 6 cal ka BP. The transportation of sediments from the abundant mafic lahar deposits was enhanced. This interval is comparable to the generally humid  $\sim 9.6$ –5.7 cal ka BP, registered in sediments from the Etzatlán-Magdalena Basin, located to the northwest of Coatetelco (Vázquez-Castro et al., 2017). This wetter interval, however, contrasts with the drier and evaporative conditions of Lake Chalco in the Basin of Mexico represented by higher carbonate (TIC) deposition (**Figure 5**; Lozano-García et al., 2015). In Lake Coatetelco, the delivery of chemically altered sediments from the watershed (PIA < 60) decreased at  $\sim 9.1$ –8.8 and  $\sim 7$ –6.5 cal ka BP. Change in provenance of sediments deposited between  $\sim 9.1$ –8.8 cal ka BP indicated possible transportation of less altered sediments from the dry watershed by aeolian activity. This arid condition and the growth interruptions in stalagmites from the nearby Cueva del Diablo and Juxtlahuaca Cave at  $\sim 8.2$  ka could be contemporary, and the chronological offset might be due to limitations of our age model (Bernal et al., 2011; Lachniet et al., 2013). The variable hydroclimate over the wetter early-to-middle Holocene was also reported by the pollen and micro-charcoal registers and magnetic susceptibility of sediments from Lake Zirahuén, located to the west of Coatetelco (Lozano-García et al., 2013). The sudden disappearance of *Alnus* in surroundings of Lake Zirahuén at  $\sim 8.2$  cal ka BP marked an arid event (**Figure 5**; Lozano-García et al., 2013). Analysis of modern and fossil diatoms along with the physico-chemical characteristics of modern-day lake water could provide additional information about paleo-pH and paleo-salinity of this phase. Similarly, the contrasting hydroclimates of Lake Coatetelco and Lake Chalco in the Basin of Mexico located at short distances from each other also need further evaluation.

#### **$\sim 6$ –2.1 cal ka BP**

Above-average water column salinity ( $\text{CaCO}_3$ ) represented generally saline conditions. Increasing *Pinus* and *Quercus* pollen along with lower *Alnus* in sediments of Lake Zirahuén suggested a trend toward drier conditions (**Figure 5**; Lozano-García et al., 2013). Below-average runoff and the deposition of sediments either without any alteration or with minimal chemical weathering represented millennial-scale droughts between  $\sim 6$  and 4.2 cal ka BP. This event is contemporary to an interval of below-average runoff and above-average salinity in the Etzatlán-Magdalena Basin (Vázquez-Castro et al., 2017). Deposition of calcite-enriched sediments represented an interval of shallow and saline water column at the coring site. Over this interval of drought-like conditions, the speleothems from Cueva del Diablo and Juxtlahuaca cave registered a wetter event, and the sediments of Etzatlán-Magdalena Basin registered more runoff at  $\sim 5$ –4 cal ka BP (Bernal et al., 2011; Vázquez-Castro et al., 2017). Absence of this event of more precipitation and the relatively lower depositional rate of 14.5 cm/ka might be indicative of another hiatus over the middle Holocene in Lake Coatetelco record. Geochemical characteristics of sediments deposited during the middle Holocene drought are comparable with sediments representing the Post-Classic drought of  $\sim 1006$ –387 cal yr BP,

contemporary with the Humo phase of pre-Columbian culture (i.e., 900–1250 CE) and abandonment of the urban center at Xochicalco (Hirth, 2000; Roy et al., 2020). Both drought intervals were characterized by lower PIA values ( $<50$ ) reflecting reduced delivery of chemically altered minerals into the lake due to lower runoff.

Runoff between above-average and below-average values and the low-to-moderate degrees of chemical alterations of deposited sediments between  $\sim 4.2$  and  $2.1$  cal ka BP represented fluctuating paleohydrology. Wetter conditions caused more erosion and deposition of moderately altered feldspars from the watershed through more runoff. Runoff decreased during the drier conditions and the silicate minerals with minimal alteration were deposited. Variable values of  $\text{Al}_2\text{O}_3$  and  $\delta^{18}\text{O}_{\text{calcite}}$  in sediments of the Aljojuca maar, located to the east of Lake Coatetelco, and variable Ti in sediments of Laguna de Juanacatlán, to the west of Coatetelco, suggest the regionally extensive nature of this unstable hydroclimate (Bhattacharya et al., 2015; Jones et al., 2015). The nearby stalagmites from Juxtlahuaca and Cueva del Diablo, however, showed trends toward drier conditions. The later part of this interval was contemporary with the earliest human influence in the surroundings. Settlements by the Olmec families post 500 BCE in the vicinity of the Lake Coatetelco and nearby streams might have occurred during this interval of unstable hydrology (e.g., Angulo, 1978; Konieczna, 1992).

## Source of Organic Matter: Aquatic vs. Terrestrial Plants

Source of the low organic matter ( $<1\%$ ) preserved in sediments of the Lake Coatetelco was interpreted cautiously as aquatic and/or terrestrial plants using the carbon to nitrogen ratios and  $\delta^{13}\text{C}_{\text{org}}$  values (e.g., Meyers and Lallier-Vergès, 1999). The organic carbon from phytoplankton, with more N-compounds, has low C/N ( $<10$ ) and the elevated values ( $10\text{--}20$ : mixed aquatic and vascular plants;  $>20$ : vascular plants) reflect higher contribution from cellulose-rich and protein-poor vascular land plants (Talbot and Johannessen, 1992; Meyers and Ishiwatari, 1993; Meyers and Lallier-Vergès, 1999). Lacustrine phytoplankton is characterized by  $\delta^{13}\text{C}_{\text{org}}$  between  $-47$  and  $-26\%$  VPDB (e.g., Smith and Winter, 1996; Leng and Marshall, 2004; Silvera et al., 2005; Cernusak et al., 2013; Crayn et al., 2015). The organic matter from terrestrial plants indicative of humid environments with  $\text{C}_3$  photosynthetic pathways has comparatively depleted  $\delta^{13}\text{C}_{\text{org}}$  compositions ( $-37$  to  $-20\%$  VPDB; mean:  $-27\%$  VPDB) and it is also more depleted compared to  $\text{C}_4$  photosynthetic pathway plants from water-deficient regions ( $\delta^{13}\text{C}_{\text{org}}$ :  $-17$  to  $-9\%$  VPDB; mean:  $-13\%$  VPDB) (Cerling et al., 1997; Kohn, 2010). The plants with Crassulacean Acid Metabolism (CAM) photosynthetic pathway, however, are difficult to identify from the carbon isotope compositions of organic matter as their  $\delta^{13}\text{C}_{\text{org}}$  values ( $-32.30$  to  $-11.80\%$  VPDB) overlap the ranges of  $\text{C}_3$  and  $\text{C}_4$  plants (Smith and Winter, 1996; Silvera et al., 2005; Cernusak et al., 2013; Crayn et al., 2015). In the Teotihuacan valley of central Mexico, the aquatic plants ( $\delta^{13}\text{C}_{\text{org}}$ :  $-30.46$  to  $-21.77\%$  VPDB) and  $\text{C}_3$  land grasses ( $-28.79$  to  $-25.63\%$  VPDB) have overlapping carbon isotope compositions

(Lounejeva-Baturina et al., 2006). Both, however, are depleted compared to the  $\text{C}_4$  land grasses ( $-14.79$  to  $-12.08\%$  VPDB) and CAM plants ( $-13.41$  to  $-13.18\%$  VPDB) from the same region. The combination of C/N ratio and  $\delta^{13}\text{C}_{\text{org}}$  deciphered the sources of organic matter deposited during the two broad paleoenvironment intervals (Figure 8).

### $\sim 11.5\text{--}6$ cal ka BP

Carbon isotope compositions ( $-25.36$  and  $-15.53\%$  VPDB) of organic matter are intermediate to the ranges of aquatic  $\text{C}_3$  plants as one end member and  $\text{C}_4$  plants as the other end member (Figure 8). They, however, were carefully evaluated with support from C/N ratios in the absence of fossil pollen data. The combination of generally lower C/N values ( $\leq 10$ ) and depleted  $\delta^{13}\text{C}_{\text{org}}$  suggest that the deposited biomass was sourced dominantly from the aquatic plants and hence, the deposition of the fine sand layer at  $\sim 11.5\text{--}11.2$  cal ka BP occurred in a lacustrine depositional environment. Below-average  $\text{CaCO}_3$  represented less saline water column during this interval of mostly autochthonous productivity. Sediments of  $\sim 10$  cal ka BP marked a notable event with C/N values of  $10\text{--}20$ , suggesting contributions from both terrestrial and aquatic plants. Higher  $\delta^{13}\text{C}_{\text{org}}$  values, however, indicated an increase in the contribution of  $\text{C}_4$  plants at the coring site (Figure 8). Moderate degrees of chemical alterations of the deposited sediments suggested transportation of more  $\text{C}_4$  plant-based organic matter occurred in wetter conditions.

### $\sim 6\text{--}2.1$ cal ka BP

Generally, higher C/N values ( $>10$ ) indicated more organic matter from the terrestrial plants, and the gradually higher  $\delta^{13}\text{C}_{\text{org}}$  reflected increasing influence of  $\text{C}_4$  vegetation. Both aquatic and terrestrial plants continued to contribute above-average TOC. Evaporative conditions and saline water column represented this interval of mixed (allochthonous and autochthonous) productivity. Variable degrees of chemical weathering of both Ti-enriched and Ti-depleted sediments along with calcite suggested fluctuating runoff and presence of a shallow water column. Contribution from the aquatic plants remained minimal during this dry interval with a depositional hiatus. The homogeneous  $\delta^{13}\text{C}_{\text{org}}$  ( $-17.21$  to  $-15.80\%$  VPDB), however, represented a generally stable environment between  $\sim 4.2\text{--}2.1$  cal ka BP and dominance of  $\text{C}_4$  grasses in the catchment (e.g., Hattersley, 1982). Better distinction within the terrestrial vegetation and aquatic plants, and their influences on the deposited organic matter, however, require studies on isotopic compositions of compound-specific biomarkers and fossil pollen (e.g., Lane et al., 2011; Lane and Horn, 2013).

## Comparison With Forcing

The modern era hydroclimate of Lake Coatetelco and its surroundings is controlled by the warm season precipitation (June–October), forced by the ENSO activity and ITCZ position (Magaña and Quintanar, 1997; Magaña, 1999; Magaña et al., 2003). During the El Niño years, the stronger easterly winds and the associated displacement of ITCZ toward southerly latitudes reduce the amounts of precipitation in the region (Magaña

et al., 2003). The reconstructed rainfall records since the LGM from the nearby speleothems were also driven by the Atlantic Meridional Overturning Circulation (AMOC) and events of ice-rafted debris into the Northern Atlantic modulating the position of ITCZ (Bernal et al., 2011; Lachniet et al., 2013). Sand content in the El Junco Lake of the Galapagos Islands and Ti values in sediments of the Cariaco Basin are the proxies for frequency-amplitude of ENSO and latitudinal shifts in mean position of the ITCZ, respectively (Haug et al., 2001; Conroy et al., 2008). Comparison with both the proxy registers helped to evaluate the forcing of ITCZ and ENSO on the paleoenvironmental and paleohydrological conditions of Lake Coatetelco (Figure 8). The summer (July) and autumn (September) insolation in orbital scale (Berger and Loutre, 1991) and the North Hemisphere temperature in millennial scale (NGRIP Project Members, 2004) are also compared in Figure 8.

Variation in the summer insolation shows a first-order negative relationship in orbital scale with the  $\delta^{13}\text{C}_{\text{org}}$  composition-based paleoenvironment. More autochthonous organic matter was deposited during the interval of higher summer insolation ( $\sim 11.5\text{--}6$  cal ka BP), and the allochthonous contribution increased during the phase of lower summer insolation ( $\sim 6\text{--}2.1$  cal ka BP). The summer insolation, however, showed orbital-scale similarity with erosion and sediment-water interactions in Lake Coatetelco watershed only up to  $\sim 4.2$  cal ka BP. More runoff of  $\sim 10.2\text{--}6$  cal ka BP was contemporary to an interval of more summer insolation and reduced runoff of  $\sim 6\text{--}4.2$  cal ka BP was coeval to an interval of less summer insolation. The ITCZ remained at northern latitudes during the wetter interval and shifted to southern latitudes as the hydroclimate became drier. The migration of ITCZ was the result of changing insolation as well as the interhemispheric temperature gradient (McGee et al., 2014, 2018). However, it is not clear what might be the forcing on an abrupt shift to drier conditions at 6 ka. The highest calcite precipitation and lowest runoff with minimal sediment-water interactions at the watershed during  $\sim 6\text{--}4.2$  cal ka BP occurred as the autumn insolation remained high (more evaporation) and summer insolation remained low (less precipitation) suggesting the possible influences of both the warm seasons' insolation on the middle Holocene drought. Reduced summer precipitation might have decreased the runoff and the enhanced evaporation of autumn possibly led to presence of a shallow and saline water column more frequently between  $\sim 6$  and 4.2 cal ka BP. This arid interval was also contemporary to some of the ice-rafted debris events into the Northern Atlantic (e.g., at  $\sim 5.9$  cal ka BP and  $\sim 4.3$  cal ka BP; Bond et al., 1997). Abrupt advection of cooler and ice-bearing surface waters from the Labrador Sea into the North Atlantic caused cooler SST (possibly  $< 2^\circ\text{C}$ ; Bond et al., 1997). The reduced formation of North Atlantic Deep Water and weak thermohaline circulation led to enhanced aridity in the nearby Cueva del Diablo (Bernal et al., 2011). The forcing of Atlantic Ocean SST on the dynamics of moisture transported into Lake Coatetelco cannot be evaluated at this stage as it requires more robust age control and records with better sediment preservation.

Over the early and middle Holocene (i.e., up to  $\sim 4.2$  cal ka BP), the paleohydrological record shows minimal similarity with the ENSO. Displacement of the ITCZ to southerly latitudes occurred during the interval of more frequent El-Niño conditions over the last  $\sim 4.2$  cal ka. However, the runoff record of Coatetelco between  $\sim 4.2$  and 2.1 cal ka BP was decoupled from the ITCZ and summer insolation. Both the erosion and sediment-water interactions remained unstable as ENSO became stronger with more frequent El-Niño (Figure 8). SST of the tropical northeast Pacific Ocean increases up to  $3^\circ\text{C}$  during the El Niño years at an interannual scale, and it forces the hurricanes to have more intense winds (De Maria and Kaplan, 1994). Magaña et al. (2003) reported  $> 20$  annual events of storms and hurricanes in the eastern Pacific during the El-Niño conditions of 1982–1983 CE and 1997–1998 CE. Hurricanes with longer durations ( $> 7$  days) were also more frequent during both years. The precipitation registered in the meteorological station at Miacatlán (at 4 km north of the lake) between 1955 and 2016 CE suggests above-average autumn precipitation and below-average total annual precipitation during both the years with El Niño conditions. Stronger ENSO and more frequent El-Niño post 4.2 cal ka BP possibly increased the frequency of short-lived tropical cyclones in an overall arid interval (e.g., Ropelewski and Halpert, 1987; Reyes and Mejía-Trejo, 1991; Englehart and Douglas, 2001; Jáuregui, 2003; Larson et al., 2005). Over this interval of increased storminess, the small groups of Olmec families established permanent sites for religious and ceremonial activities, as well as several commercial exchange centers in the area surrounding Lake Coatetelco. Occupation around the Coatán Viejo site and on the banks of Chalma, Amacuzac, and Tembembe rivers commenced at  $\sim 500$  BCE in an interval of more water availability, at least during part of the year, due to frequent storms (e.g., Hirth, 2010). The exact relationship between earliest human occupations in this region and climate, however, needs further evaluation (Angulo, 1978; Konieczna, 1992). This interval of unstable hydrology was also documented at the Etzatlán-Magdalena Basin of western Mesoamerica through variable lake water salinity and chemical alteration caused from more hurricane activity in the eastern Pacific (Vázquez-Castro et al., 2017). Dissimilarities in trends of our lacustrine register and the records of oxygen isotope compositions of speleothems from Juxtlahuaca Cave and Cueva del Diablo might indicate different sensitivities of both the geological records to the seasonal and annual precipitation and near-surface processes like erosion in response to global climate change.

## CONCLUSION

A new sedimentary record from Lake Coatetelco (southwest Mexico) helped to extend the paleoenvironmental information of central Mesoamerica and complemented the existing paleoclimate data by reconstructing the sources of deposited organic matter and responses of precipitation-evaporation under varying seasonal insolation, ITCZ positions, and ENSO activity between the earliest Holocene and the initial phase of the settled

Olmec societies (i.e., ~11.5–2.1 cal ka BP). The main conclusions of this study are as follows:

(i) Geochemical characteristics broadly deciphered two intervals of distinct paleoenvironment modulated by the summer insolation in orbital scale, i.e., ~10.2–6 cal ka BP and ~6–4.2 cal ka BP. Lower sedimentation represented a depositional hiatus between ~11.2–10.2 cal ka BP. Sediments of ~11.5–11.2 cal ka BP, ~9.1–8.8 cal ka BP and ~7–6.5 cal ka BP represented the other sub-millennial-scale arid conditions.

(ii) Generally lower C/N ( $\leq 10$ ) and depleted  $\delta^{13}\text{C}_{\text{org}}$  suggested more contribution from the aquatic plants during ~11.5–6 cal ka BP. Sediments of ~10 cal ka BP represented an event of  $\text{C}_4$  grass dominance. Influence of  $\text{C}_4$  vegetation gradually increased during ~6–2.1 cal ka BP and the homogeneous  $\delta^{13}\text{C}_{\text{org}}$  (–17.21 to –15.80‰ VPDB) between ~4.2–2.1 cal ka BP represented an interval of stable paleoenvironment.

(iii) The middle Holocene drought of ~6–4.2 cal ka BP was represented by deposition of unaltered to low degree of chemically altered siliciclastic fractions and deposition of abundant authigenic  $\text{CaCO}_3$ . Summer insolation remained low, autumn insolation was high and the ITCZ shifted to southern latitudes during this interval of frequent drought-like conditions.

(iv) Fluctuating paleohydrology of ~4.2–2.1 cal ka BP represented an unstable hydroclimate that continued until the first settlements by the Olmec families. More frequent El Niño conditions possibly increased water availability through the short-lived tropical cyclones. Dissimilarity in the trend of this lacustrine register and the oxygen isotope compositions of nearby speleothems might indicate different sensitivities of the geological records to changes in seasonal and annual precipitation and near-surface processes in response to the global climate change.

## DATA AVAILABILITY STATEMENT

The raw data supporting the conclusions of this article will be made available by the authors, without undue reservation.

## REFERENCES

- Alvarado, C. I., and Garza, S. (2010). El carácter defensivo de xochicalco (650-1 100 d. C.). *Arqueología* 43, 136–154.
- Angulo, J. (1978). *El Museo de Cuahutetelco: Guía Oficial*. Ciudad de México: Instituto Nacional de Antropología e Historia.
- Angulo, J. (2010). “Sobre la presencia olmeca y otros grupos etnolingüísticos en la región de Morelos y el Altiplano Central durante el preclásico medio y superior,” in *Historia de Morelos; Tierra, gente, tiempos del Sur: La arqueología en Morelos: Dinámicas sociales sobre las construcciones de la cultura material*, Vol. 2, eds V. López and L. Sandra (Cuernavaca: Congreso del Estado de Morelos-LI Legislatura / Universidad Autónoma del Estado de Morelos / Ayuntamiento de Cuernavaca / Instituto de Cultura de Morelos), 320.
- Aragón-Moreno, A. A., Islebe, G. A., and Torrescano-Valle, N. (2012). A ~ 3800-yr, high-resolution record of vegetation and climate change on the north coast of the Yucatan Peninsula. *Rev. Palaeobot. Palynol.* 178, 35–42. doi: 10.1016/j.revpalbo.2012.04.002
- Aragón-Moreno, A. A., Islebe, G. A., Roy, P. D., Torrescano-Valle, N., and Mueller, A. D. (2018). Climate forcings on vegetation of the southeastern Yucatan Peninsula (Mexico) during the middle to late holocene. *Palaeogeogr. Palaeoclimatol. Palaeoecol.* 495, 214–226. doi: 10.1016/j.palaeo.2018.01.014

## AUTHOR CONTRIBUTIONS

OG-A and PR contributed to the conception and design of the study, generated and collected the research data, evaluated and processed the data for interpretations, wrote the first draft, and revised and edited the reviewed manuscript. IV-M curated the cores, processed samples for the geochemical analysis, and wrote a section. MG-G carried out the XRF and mineralogical analyses and wrote a section of the manuscript. JC contributed with stable isotope analysis and wrote a section. II-A and JQ-J contributed with the age model and interpretations. All authors contributed to manuscript revision, read, and approved the submitted version.

## FUNDING

Data presented in the manuscript were funded by the Support Program for Research and Technological Innovation Projects of DGAPA-UNAM through the proposal PAPIIT-IN101121 to PR. OG-A acknowledges Posgrado en Ciencias del Mar y Limnología (UNAM) and Ph.D. scholarship from CONACyT (928976).

## ACKNOWLEDGMENTS

Jose Luis Sánchez helped in fieldwork and the core was collected by Corporación Ambiental de México (Gabriela Pantoja and Mari Cruz Trejo). The suggestions and comments from both reviewers and the editor are thankfully acknowledged.

## SUPPLEMENTARY MATERIAL

The Supplementary Material for this article can be found online at: <https://www.frontiersin.org/articles/10.3389/fevo.2022.809949/full#supplementary-material>

- Arce, J. L., Layer, P. W., Lassiter, J. C., Benowitz, J. A., Macías, J. L., and Ramírez-Espinosa, J. (2013). 40 Ar/39 Ar dating, geochemistry, and isotopic analyses of the quaternary chichinautzin volcanic field, south of Mexico City: implications for timing, eruption rate, and distribution of volcanism. *Bull. Volcanol.* 75, 774. doi: 10.1007/s00445-013-0774-6
- Berger, A., and Loutre, M.-F. (1991). Insolation values for the climate of the last 10 million years. *Quat. Sci. Rev.* 10, 297–317. doi: 10.1016/0277-3791(91)90033-Q
- Bernal, J. P., Lachniet, M., McCulloch, M., Mortimer, G., Morales, P., and Cienfuegos, E. (2011). A speleothem record of holocene climate variability from southwestern Mexico. *Quat. Res.* 75, 104–113. doi: 10.1016/j.yqres.2010.09.002
- Bhattacharya, T., Byrre, R., Böhnell, H., Wogau, K., Kienel, U., Ingram, B. L., et al. (2015). Cultural implications of late holocene climate change in the Cuenca Oriental, Mexico. *Proc. Natl Acad. Sci. U.S.A.* 112, 1693–1698. doi: 10.1073/pnas.1405653112
- Bond, G., Showers, W., Cheseby, M., Lotti, R., Almasi, P., DeMenocal, P., et al. (1997). A pervasive millennial-scale cycle in North Atlantic holocene and glacial climates. *Science* 278, 1257–1266. doi: 10.1126/science.278.5341.1257
- Bradbury, J. P. (2000). Limnologic history of Lago de Patzcuaro, Michoacan, Mexico for the past 48,000 years: impacts of climate and man. *Palaeogeogr. Palaeoclimatol. Palaeoecol.* 163, 69–95. doi: 10.1016/S0031-0182(00)00146-2

- Bronk Ramsey, C. (2008). Deposition models for chronological records. *Quat. Sci. Rev.* 27, 42–60. doi: 10.1016/j.quascirev.2007.01.019
- Bronk Ramsey, C. (2009). Bayesian analysis of radiocarbon dates. *Radiocarbon* 51, 337–360. doi: 10.1038/s41586-020-2343-4
- Bronk Ramsey, C., and Lee, S. (2013). Recent and planned developments of the program OxCal. *Radiocarbon* 55, 720–730. doi: 10.1017/S003382200057878
- Camuti, K. S., and McGuire, P. T. (1999). Preparation of polished thin sections from poorly consolidated regolith and sediment materials. *Sediment. Geol.* 128, 171–178. doi: 10.1016/S0037-0738(99)00073-1
- Carrillo-Bastos, A., Islebe, G. A., Torrescano-Valle, N., and González, N. E. (2010). Holocene vegetation and climate history of central Quintana Roo, Yucatán Peninsula, Mexico. *Rev. Palaeobot. Palynol.* 160, 189–196. doi: 10.1016/j.revpalbo.2010.02.013
- Cerling, T. E., Harris, J. M., MacFadden, B. J., Leakey, M. G., Quade, J., Eisenmann, V., et al. (1997). Global vegetation change through the miocene/pliocene boundary. *Nature* 389, 153–158. doi: 10.1007/s00114-008-0500-y
- Cernusak, L. A., Ubierna, N., Winter, K., Holtum, J. A., Marshall, J. D., and Farquhar, G. D. (2013). Environmental and physiological determinants of carbon isotope discrimination in terrestrial plants. *New Phytol.* 200, 950–965. doi: 10.1111/nph.12423
- Cohen, A. S. (2003). *Paleolimnology: The History and Evolution of Lake Systems*. New York, NY: Oxford University Press. doi: 10.1093/oso/9780195133530.001.0001
- Conroy, J. L., Overpeck, J. T., Cole, J. E., Shanahan, T. M., and Steinitz-Kannan, M. (2008). Holocene changes in eastern tropical Pacific climate inferred from a Galápagos lake sediment record. *Quat. Sci. Rev.* 27, 1166–1180. doi: 10.1016/j.quascirev.2008.02.015
- Contreras-MacBeath, T., Monroy, F. J., and Delgado, J. C. B. (2004). *La Diversidad Biológica en Morelos: Estudio del Estado*. México City: Comisión Nacional para el Conocimiento y Uso de la Biodiversidad y Universidad Autónoma del Estado de Morelos.
- Crayn, D. M., Winter, K., Schulte, K., and Smith, J. A. C. (2015). Photosynthetic pathways in bromeliaceae: phylogenetic and ecological significance of CAM and C3 based on carbon isotope ratios for 1893 species. *Bot. J. Linn. Soc.* 178, 169–221. doi: 10.1111/boj.12275
- Curtis, J. H., Hodell, D. A., and Brenner, M. (1996). Climate variability on the Yucatan Peninsula (Mexico) during the past 3500 years, and implications for Maya cultural evolution. *Quat. Res.* 46, 37–47. doi: 10.1006/qres.1996.0042
- De Maria, M., and Kaplan, J. (1994). Sea surface temperature and the maximum intensity of Atlantic tropical cyclones. *J. Clim.* 7, 1324–1334. doi: 10.1175/1520-0442(1994)007<1324:SSTATM>2.0.CO;2
- Díaz-Vargas, M., Molina-Astudillo, F. I., García-Rodríguez, J., and Elizalde-Arriaga, E. (2017). Estado trófico del lago Coatetelco, Morelos, México. *Investig. Agropecuaria* 14, 145–152.
- Diez, D. (1933). *Bibliografía del Estado de MORELOS*. México City: Imprenta de la Secretaría de relaciones exteriores.
- Englehart, P. J., and Douglas, A. V. (2001). The role of eastern North Pacific tropical storms in the rainfall climatology of western Mexico. *Int. J. Climatol.* 21, 1357–1370. doi: 10.1002/joc.637
- Fedo, C. M., Wayne Nesbitt, H., and Young, G. M. (1995). Unraveling the effects of potassium metasomatism in sedimentary rocks and paleosols, with implications for paleoweathering conditions and provenance. *Geology* 23, 921–924. doi: 10.1130/0091-7613(1995)023<0921:UTEOPM>2.3.CO;2
- Fries, C. (1960). *Geología del Estado de Morelos y de Partes Adyacentes de México y Guerrero, Región Central Meridional de México*. Mexico City: Universidad Nacional Autónoma de México.
- Gómez-Márquez, J. L. (2002). *Estudio limnológico-pesquero del lago de Coatetelco, Morelos, México* [PhD thesis]. Tesis de Doctorado en Ciencias (Biología), Facultad de Ciencias. Ciudad de México: UNAM.
- González, N., and Garza, S. (1994). Xochicalco. *Arqueol. Mex.* 2, 70–74.
- Grove, D. C. (2010). “Morelos, la cuna de la famosa cultura de Tlatilco (1200–900 a.C.)” in *Historia de Morelos: Tierra, Gente, Tiempos del Sur: la Arqueología en Morelos: Dinámicas Sociales Sobre las Construcciones de la Cultura Material*, eds V. López and L. Sandra (Cuernavaca: Congreso del Estado de Morelos-LI Legislatura / Universidad Autónoma del Estado de Morelos / Ayuntamiento de Cuernavaca / Instituto de Cultura de Morelos), 320.
- Hattersley, P. W. (1982).  $\Delta^{13}$  values of C4 types in grasses. *Funct. Plant Biol.* 9, 139–154. doi: 10.1071/PP9820139
- Haug, G. H., Günther, D., Peterson, L. C., Sigman, D. M., Hughen, K. A., and Aeschlimann, B. (2003). Climate and the collapse of Maya civilization. *Science* 299, 1731–1735. doi: 10.1126/science.1080444
- Haug, G. H., Hughen, K. A., Sigman, D. M., Peterson, L. C., and Röhl, U. (2001). Southward migration of the intertropical convergence zone through the holocene. *Science* 293, 1304–1308. doi: 10.1126/science.1059725
- Hirth, K. (2000). *Ancient Urbanism at Xochicalco: The Evolution and Organization of a Pre-Hispanic Society*, Salt Lake City, UT: University of Utah Press.
- Hirth, K. G. (2010). “De teotihuacán a Xochicalco: los periodos clásico y epiclásico en Morelos, in *Historia de Morelos: Tierra, Gente, Tiempos del Sur: la Arqueología en Morelos: Dinámicas Sociales Sobre las Construcciones de la Cultura Material*, eds V. López and L. Sandra (Cuernavaca: Congreso del Estado de Morelos-LI Legislatura / Universidad Autónoma del Estado de Morelos / Ayuntamiento de Cuernavaca / Instituto de Cultura de Morelos), 320.
- Hodell, D. A., Brenner, M., and Curtis, J. H. (2005). Terminal Classic drought in the northern Maya lowlands inferred from multiple sediment cores in Lake Chichancanab (Mexico). *Quat. Sci. Rev.* 24, 1413–1427. doi: 10.1016/j.quascirev.2004.10.013
- Hodell, D. A., Brenner, M., Curtis, J. H., and Guilderson, T. (2001). Solar forcing of drought frequency in the Maya lowlands. *Science* 292, 1367–1370. doi: 10.1126/science.1057759
- Jáuregui, E. (2003). Climatology of landfalling hurricanes and tropical storms in Mexico. *Atmósfera* 16, 193–204.
- Jennerjahn, T. C., Ittekkot, V., Arz, H. W., Behling, H., Pätzold, J., and Wefer, G. (2004). Asynchronous terrestrial and marine signals of climate change during Heinrich events. *Science* 306, 2236–2239. doi: 10.1126/science.1102490
- Jones, M. D., Metcalfe, S. E., Davies, S. J., and Noren, A. (2015). Late holocene climate reorganisation and the north American monsoon. *Quat. Sci. Rev.* 124, 290–295. doi: 10.1016/j.quascirev.2015.07.004
- Kohn, M. J. (2010). Carbon isotope compositions of terrestrial C3 plants as indicators of (paleo) ecology and (paleo) climate. *Proc. Natl. Acad. Sci. U.S.A.* 107, 19691–19695. doi: 10.1073/pnas.1004933107
- Konieczna, B. (1992). *Coatetelco, Morelos: Mini-Guia*. Mexico City: Instituto Nacional de Antropología e Historia.
- Lachniet, M. S., Asmerom, Y., Bernal, J. P., Polyak, V. J., and Vazquez-Selem, L. (2013). Orbital pacing and ocean circulation-induced collapses of the Mesoamerican monsoon over the past 22,000 y. *Proc. Natl. Acad. Sci. U.S.A.* 110, 9255–9260. doi: 10.1073/pnas.1222804110
- Lachniet, M. S., Asmerom, Y., Polyak, V., and Bernal, J. P. (2017). Two millennia of Mesoamerican monsoon variability driven by Pacific and Atlantic synergistic forcing. *Quat. Sci. Rev.* 155, 100–113. doi: 10.1016/j.quascirev.2016.11.012
- Lane, C. S., and Horn, S. P. (2013). Terrestrially derived n-alkane  $\delta D$  evidence of shifting holocene paleohydrology in highland Costa Rica. *Arct. Antarct. Alp. Res.* 45, 342–349. doi: 10.1657/1938-4246-45.3.342
- Lane, C. S., Horn, S. P., Mora, C. I., Orvis, K. H., and Finkelstein, D. B. (2011). Sedimentary stable carbon isotope evidence of late quaternary vegetation and climate change in highland Costa Rica. *J. Paleolimnol.* 45, 323–338. doi: 10.1007/s10933-011-9500-6
- Larson, J., Zhou, Y., and Higgins, R. W. (2005). Characteristics of landfalling tropical cyclones in the United States and Mexico: climatology and interannual variability. *J. Clim.* 18, 1247–1262. doi: 10.1175/JCLI3317.1
- Leng, M. J., and Marshall, J. D. (2004). Palaeoclimate interpretation of stable isotope data from lake sediment archives. *Quat. Sci. Rev.* 23, 811–831. doi: 10.1016/j.jhevol.2010.05.006
- Lounejeva-Baturina, E., Morales Puente, P., Cabadas Báez, H. V., Cienfuegos Alvarado, E., Sedov, S., Vallejo Gómez, E., et al. (2006). Late pleistocene to holocene environmental changes from  $\delta^{13}C$  determinations in soils at Teotihuacan, Mexico. *Geofis. Int.* 45, 85–98. doi: 10.22201/igeof.00167169p.2006.45.2.184
- Lozano-García, S., Caballero, M., Ortega, B., Rodríguez, A., and Sosa, S. (2007). Tracing the effects of the little Ice Age in the tropical lowlands of eastern Mesoamerica. *Proc. Natl. Acad. Sci. U.S.A.* 104, 16200–16203. doi: 10.1073/pnas.0707896104
- Lozano-García, S., Ortega, B., Roy, P. D., Beramendi-Orosco, L., and Caballero, M. (2015). Climatic variability in the northern sector of the American tropics since the latest MIS 3. *Quat. Res.* 84, 262–271. doi: 10.1016/j.yqres.2015.07.002

- Lozano-García, S., Torres-Rodríguez, E., Ortega, B., Vázquez, G., and Caballero, M. (2013). Ecosystem responses to climate and disturbances in western central Mexico during the late Pleistocene and holocene. *Palaeogeogr. Palaeoclimatol. Palaeoecol.* 370, 184–195. doi: 10.1016/j.palaeo.2012.12.006
- Magaña, V. (1999). “El Clima y El Niño,” in *Los Impactos de El Niño en México*, ed. V. Magaña (México City: Dirección General de Protección Civil, Secretaría de Gobernación). doi: 10.12933/therya-19-899
- Magaña, V. O., Vázquez, J. L., Pérez, J. L., and Pérez, J. B. (2003). Impact of El Niño on precipitation in Mexico. *Geofis. Int.* 42, 313–330. doi: 10.22201/igeof.00167169p.2003.42.2.269
- Magaña, V., and Quintanar, A. I. (1997). “On the use of general circulation models to study regional climate,” in *Proceedings of the 2nd UNAM-CRAY Supercomputing Conference* (Cambridge: Cambridge University Press).
- Maldonado, D. (2005). *Religiosidad indígena. Historia y Etnografía de Coatepec, Morelos*. Ciudad de México: INAH.
- Mazari, M. (1986). *Bosquejo Histórico del Estado de Morelos*. Chamilpa: Universidad Autónoma del Estado de Morelos.
- McGee, D., Donohoe, A., Marshall, J., and Ferreira, D. (2014). Changes in ITCZ location and cross-equatorial heat transport at the last glacial maximum, Heinrich Stadial 1, and the mid-Holocene. *Earth Planet. Sci. Lett.* 390, 69–79. doi: 10.1016/j.epsl.2013.12.043
- McGee, D., Moreno-Chamarro, E., Green, B., Marshall, J., Galbraith, E., and Bradtmiller, L. (2018). Hemispherically asymmetric trade wind changes as signatures of past ITCZ shifts. *Quate. Sci. Rev.* 180, 214–228. doi: 10.1016/j.quascirev.2017.11.020
- Medina-Elizalde, M., Burns, S. J., Lea, D. W., Asmerom, Y., von Gunten, L., Polyak, V., et al. (2010). High resolution stalagmite climate record from the Yucatán Peninsula spanning the Maya terminal classic period. *Earth Planet. Sci. Lett.* 298, 255–262. doi: 10.1016/j.epsl.2010.08.016
- Metcalfe, S. E., Jones, M. D., Davies, S. J., Noren, A., and MacKenzie, A. (2010). Climate variability over the last two millennia in the North American Monsoon region, recorded in laminated lake sediments from Laguna de Juanacatlán, Mexico. *Holocene* 20, 1195–1206. doi: 10.1177/0959683610371994
- Meyers, P. A., and Ishiwatari, R. (1993). Lacustrine organic geochemistry—an overview of indicators of organic matter sources and diagenesis in lake sediments. *Organ. Geochem.* 20, 867–900. doi: 10.1016/0146-6380(93)90100-P
- Meyers, P. A., and Lallier-Vergès, E. (1999). Lacustrine sedimentary organic matter records of late quaternary paleoclimates. *J. Paleolimnol.* 21, 345–372. doi: 10.1023/A:1008073732192
- Nesbitt, H. W., and Young, G. M. (1984). Prediction of some weathering trends of plutonic and volcanic rocks based on thermodynamic and kinetic considerations. *Geochim. Cosmochim. Acta* 48, 1523–1534. doi: 10.1016/0016-7037(84)90408-3
- Nesbitt, H. W., and Young, G. M. (1989). Formation and diagenesis of weathering profiles. *J. Geol.* 97, 129–147. doi: 10.1086/629290
- NGRIP Project Members. (2004). High-resolution record of Northern Hemisphere climate extending into the last interglacial period. *Nature* 431, 147–151. doi: 10.1038/nature02805
- Park, J., Byrne, R., and Böhnell, H. (2019). Late holocene climate change in Central Mexico and the decline of Teotihuacan. *Ann. Am. Assoc. Geogr.* 109, 104–120. doi: 10.1080/24694452.2018.1488577
- Parkhurst, D. L., and Appelo, C. A. J. (2013). Description of input and examples for PHREEQC version 3—a computer program for speciation, batch-reaction, one-dimensional transport, and inverse geochemical calculations. *U.S. Geol. Surv. Techniques Methods* 6:A43. doi: 10.3133/tm6A43
- Reimer, P. J., Austin, W. E., Bard, E., Bayliss, A., Blackwell, P. G., Ramsey, C. B., et al. (2020). The IntCal20 Northern Hemisphere radiocarbon age calibration curve (0–55 cal kBP). *Radiocarbon* 62, 725–757. doi: 10.1017/RDC.2020.41
- Reyes, S., and Mejía-Trejo, A. (1991). Tropical perturbations in the Eastern Pacific and the precipitation field over North-Western Mexico in relation to the Enso phenomenon. *Int. J. Climatol.* 11, 515–528. doi: 10.1002/joc.3370110505
- Ropelewski, C. F., and Halpert, M. S. (1987). Global and regional scale precipitation patterns associated with the El Niño/Southern Oscillation. *Mon. Weather Rev.* 115, 1606–1626. doi: 10.1175/1520-0493(1987)115<1606:GARSPP>2.0.CO;2
- Roy, P. D., Arce, J. S., Lozano, R., Jonathan, M. P., Centeno-García, E., and Lozano-García, S. (2012). Geochemistry of a tephra-paleosol sequence from north-eastern Basin of Mexico: implications to tephrochronology and chemical weathering during quaternary. *Rev. Mex. Cienc. Geol.* 29, 24–38.
- Roy, P. D., Caballero, M., Lozano, R., and Smykatz-Kloss, W. (2008). Geochemistry of late quaternary sediments from Tecocomulco lake, central Mexico: implication to chemical weathering and provenance. *Geochemistry* 68, 383–393. doi: 10.1016/j.chemer.2008.04.001
- Roy, P. D., García-Arriola, O. A., Garza-Tarazon, S., Vargas-Martínez, I. G., Muthusankar, G., Giron-García, P., et al. (2020). Late Holocene depositional environments of Lake Coatetelco in Central-Southern Mexico and comparison with cultural transitions at Xochicalco. *Palaeogeogr. Palaeoclimatol. Palaeoecol.* 560:110050. doi: 10.1016/j.palaeo.2020.110050
- Roy, P. D., Torrescano-Valle, N., Islebe, G. A., and Gutiérrez-Ayala, L. V. (2017). Late holocene hydroclimate of the western Yucatan Peninsula (Mexico). *J. Quat. Sci.* 32, 1112–1120. doi: 10.1002/jqs.2988
- Shao, J., Yang, S., and Li, C. (2012). Chemical indices (CIA and WIP) as proxies for integrated chemical weathering in China: inferences from analysis of fluvial sediments. *Sediment. Geol.* 265–266, 110–120. doi: 10.1016/j.sedgeo.2012.03.020
- Silvera, K., Santiago, L. S., and Winter, K. (2005). Distribution of crassulacean acid metabolism in orchids of Panama: evidence of selection for weak and strong modes. *Funct. Plant Biol.* 32, 397–407. doi: 10.1071/FP04179
- Smith, J. A. C., and Winter, K. (1996). “Taxonomic distribution of crassulacean acid metabolism,” in *En Crassulacean acid Metabolism*, eds K. Winter and J. A. C. Smith (Berlin: Springer), 427–436. doi: 10.1007/978-3-642-79060-7\_27
- Smith, M. E. (2010). “La época posclásica en Morelos: surgimiento de los tlahuicas y xochimilcas,” in *Historia de Morelos; Tierra, Gente, Tiempos del Sur: La Arqueología en Morelos. Dinámicas Sociales Sobre las Construcciones de la Cultura Material*, Vol. 2, eds V. López and L. Sandra (Cuernavaca: Congreso del Estado de Morelos-LI Legislatura / Universidad Autónoma del Estado de Morelos / Ayuntamiento de Cuernavaca / Instituto de Cultura de Morelos):320.
- Stuart, G. (2003). *Pre-Hispanic Sociopolitical Development and Wetland Agriculture in the Tequila Valleys of West Mexico*. Tempe, AZ: Arizona State University.
- Talbot, M. R., and Johannessen, T. (1992). A high resolution palaeoclimatic record for the last 27,500 years in tropical West Africa from the carbon and nitrogen isotopic composition of lacustrine organic matter. *Earth Planet. Sci. Lett.* 110, 23–37. doi: 10.1016/0012-821X(92)90036-U
- Vázquez-Castro, G., Roy, P. D., and Solís-Castillo, B. (2019). Geochemical evidence of anthropogenic activity in western Mesoamerica since the classic period. *J. Archaeol. Sci. Rep.* 26:101920. doi: 10.1016/j.jasrep.2019.101920
- Vázquez-Castro, G., Roy, P. D., Solís, B., Blanco, E., and Lozano-Santacruz, R. (2017). Holocene paleohydrology of the Etzatlán-Magdalena basin in western-central Mexico and evaluation of main atmospheric forcings. *Palaeogeogr. Palaeoclimatol. Palaeoecol.* 487, 149–157. doi: 10.1016/j.palaeo.2017.08.029
- Webb, R. W., and Hirth, K. G. (2000). Rapidly abandoned households at Xochicalco, Morelos, Mexico. *Mayab* 13, 88–102.

**Conflict of Interest:** The authors declare that the research was conducted in the absence of any commercial or financial relationships that could be construed as a potential conflict of interest.

**Publisher’s Note:** All claims expressed in this article are solely those of the authors and do not necessarily represent those of their affiliated organizations, or those of the publisher, the editors and the reviewers. Any product that may be evaluated in this article, or claim that may be made by its manufacturer, is not guaranteed or endorsed by the publisher.

Copyright © 2022 García-Arriola, Roy, Vargas-Martínez, Giron-García, Curtis, Israde-Alcantara and Quiroz-Jimenez. This is an open-access article distributed under the terms of the Creative Commons Attribution License (CC BY). The use, distribution or reproduction in other forums is permitted, provided the original author(s) and the copyright owner(s) are credited and that the original publication in this journal is cited, in accordance with accepted academic practice. No use, distribution or reproduction is permitted which does not comply with these terms.